2019-12

A DECADAL COMPARISON OF THE ARCTIC UPPER OCEAN HEAT CONTENT IN THE BEAUFORT SEA AND TRANSPOLAR DRIFT

Albee, Roslyn E.

Monterey, CA; Naval Postgraduate School

NAVAL POSTGRADUATE SCHOOL

MONTEREY, CALIFORNIA

THESIS

A DECADAL COMPARISON OF THE ARCTIC UPPER OCEAN HEAT CONTENT IN THE BEAUFORT SEA AND TRANSPOLAR DRIFT

by

Roslyn E. Albee

December 2019

Thesis Advisor: Timothy P. Stanton
Co-Advisor: William J. Shaw

Approved for public release. Distribution is unlimited.

THIS PAGE INTENTIONALLY LEFT BLANK

REPORT DOCUMENTATION PAGE			*Form Approved OMB No. 0704-0188*

1. AGENCY USE ONLY *(Leave blank)*	**2. REPORT DATE** December 2019	**3. REPORT TYPE AND DATES COVERED** Master's thesis

4. TITLE AND SUBTITLE
A DECADAL COMPARISON OF THE ARCTIC UPPER OCEAN HEAT CONTENT IN THE BEAUFORT SEA AND TRANSPOLAR DRIFT

5. FUNDING NUMBERS

6. AUTHOR(S) Roslyn E. Albee

7. PERFORMING ORGANIZATION NAME(S) AND ADDRESS(ES)
Naval Postgraduate School
Monterey, CA 93943-5000

8. PERFORMING ORGANIZATION REPORT NUMBER

9. SPONSORING / MONITORING AGENCY NAME(S) AND ADDRESS(ES)
N/A

10. SPONSORING / MONITORING AGENCY REPORT NUMBER

11. SUPPLEMENTARY NOTES The views expressed in this thesis are those of the author and do not reflect the official policy or position of the Department of Defense or the U.S. Government.

12a. DISTRIBUTION / AVAILABILITY STATEMENT
Approved for public release. Distribution is unlimited.

12b. DISTRIBUTION CODE
A

13. ABSTRACT (maximum 200 words)

The Arctic has had a strong response to global climate change expressed through widespread melting of the perennial ice cover in the Canada Basin at an increasing rate. High resolution coupled atmospheric and ocean climate models significantly underestimate this reduction in late summer ice extent. In this study, long term ocean time series observations from ice tethered profilers (ITPs) and autonomous ocean flux buoys (AOFBs) enable the integration of upper ocean temperature structure to make estimates of ocean mixed layer heat content over seasonal time scales. Advanced Microwave Scanning Radiometer (AMSR) data are used to estimate open water fraction, which is a strong driver of ocean heating in the late summer. A primary hypothesis of this study is that there will be a significant difference in late summer ocean mixed layer heat content between the Beaufort Sea and the more convergent Transpolar Drift. The higher open water fraction increases the amount of solar radiation inputs into the upper ocean in the Beaufort Sea.

14. SUBJECT TERMS ocean heat content, Arctic Ocean, ocean mixed layer, Beaufort Gyre, Beaufort Sea, transpolar drift, temperature, salinity, density, stratified ocean dynamics of the Arctic, SODA, open water fraction	**15. NUMBER OF PAGES** 73
	16. PRICE CODE

17. SECURITY CLASSIFICATION OF REPORT	**18. SECURITY CLASSIFICATION OF THIS PAGE**	**19. SECURITY CLASSIFICATION OF ABSTRACT**	**20. LIMITATION OF ABSTRACT**
Unclassified	Unclassified	Unclassified	UU

NSN 7540-01-280-5500

Standard Form 298 (Rev. 2-89)
Prescribed by ANSI Std. 239-18

THIS PAGE INTENTIONALLY LEFT BLANK

Approved for public release. Distribution is unlimited.

A DECADAL COMPARISON OF THE ARCTIC UPPER OCEAN HEAT CONTENT IN THE BEAUFORT SEA AND TRANSPOLAR DRIFT

Roslyn E. Albee
Lieutenant, United States Navy
BS, Oregon State University, 2013

Submitted in partial fulfillment of the
requirements for the degree of

MASTER OF SCIENCE IN METEOROLOGY AND PHYSICAL OCEANOGRAPHY

from the

NAVAL POSTGRADUATE SCHOOL
December 2019

Approved by: Timothy P. Stanton
Advisor

William J. Shaw
Co-Advisor

Peter C. Chu
Chair, Department of Oceanography

THIS PAGE INTENTIONALLY LEFT BLANK

ABSTRACT

The Arctic has had a strong response to global climate change expressed through widespread melting of the perennial ice cover in the Canada Basin at an increasing rate. High resolution coupled atmospheric and ocean climate models significantly underestimate this reduction in late summer ice extent. In this study, long term ocean time series observations from ice tethered profilers (ITPs) and autonomous ocean flux buoys (AOFBs) enable the integration of upper ocean temperature structure to make estimates of ocean mixed layer heat content over seasonal time scales. Advanced Microwave Scanning Radiometer (AMSR) data are used to estimate open water fraction, which is a strong driver of ocean heating in the late summer. A primary hypothesis of this study is that there will be a significant difference in late summer ocean mixed layer heat content between the Beaufort Sea and the more convergent Transpolar Drift. The higher open water fraction increases the amount of solar radiation inputs into the upper ocean in the Beaufort Sea.

THIS PAGE INTENTIONALLY LEFT BLANK

TABLE OF CONTENTS

LIST OF FIGURES

LIST OF TABLES

THIS PAGE INTENTIONALLY LEFT BLANK

LIST OF ACRONYMS AND ABBREVIATIONS

AFL	Albedo Feedback Loop
AMSR	Advanced Microwave Scanning Radiometer-Earth Observing System
BG	Beaufort Gyre
CNO	Chief of Naval Operations
CTD	Conductivity-Temperature-Depth
DRI	Department Research Initiative
TDF	Temperature Departure From Freezing Point
deg C	Degrees Centigrade
HC	Heat Content
ICEX	Ice Exercise
IOBL	Ice Ocean Boundary Layer
ITP	Ice Tethered Profiler
MOSAiC	Multidisciplinary drifting Observatory for the Study of Arctic Climate
MJ	Megajoules
ML	Mixed Layer
MLD	Mixed Layer Depth
NaN	Not a Number
NAR	Navy Arctic Roadmap
NCCR	Navy Climate Change Roadmap
NPEO	North Pole Environmental Observatory
NPS	Naval Postgraduate School
NSF	National Science Foundation
NSIDC	National Snow and Ice Data Center
NSTM	Near Surface Temperature Maximum
ONR	Office of Naval Research
OWF	Open Water Fraction
psu	Practical Salinity Unit(s)
SAR	Synthetic Aperture Radar

SHEBA	Surface Heat Budget of the Arctic
sML	Summer mixed layer
SODA	Stratified Ocean Dynamics in the Arctic
T/C	Temperature/Conductivity
T/S	Temperature/Salinity
TFCC	Task Force Climate Change
TPD	Transpolar Drift
USCGC	United States Coast Guard Cutter (USCGC)
WHOI	Woods Hole Oceanographic Institute
WML	Winter Mixed Layer

ACKNOWLEDGMENTS

Advisor: Professor Tim Stanton

Co-advisor: Professor Bill Shaw

USCGC Healy

Office of Naval Research (ONR)

NPS METOC December 2019 Cohort

Family (Dad, Mom, Raquel)

Lab colleagues (Terrance and Amanda)

THIS PAGE INTENTIONALLY LEFT BLANK

I. INTRODUCTION

A. ARCTIC CHANGE IMPACTS ON THE NAVY AND SOCIETY

The United States has a strategically important vested interest in the Arctic. The transportation industry may soon see a reduction in travel time as new shipping routes open in the Arctic Ocean. Additional opportunities for natural resources including oil will become accessible. Naval importance is shown through increased Office of Naval Research (ONR) funding and Task Forces in the region along with the interest of other countries. The Navy established Task Force Climate Change (TFCC) in 2009 producing both the *Navy Arctic Roadmap (NAR)* and *Navy Climate Change Roadmap (NCCR)* documents (TFCC 2009). The Chief of Naval Operations (CNO) then released *The United States Navy Arctic Roadmap for 2014 to 2030* highlighting the need to improve environmental understanding for future Arctic operations (TFCC 2014). Ongoing Naval ice operations in the Arctic such as Ice Exercise (ICEX) emphasis the central role of the Arctic in submarine warfare.

Response of the Arctic to climate change is more drastic than at lower latitudes. The implications are far reaching globally such as increased solar radiation energy into the ocean and land, and decreased sea ice thickness and extent. There are a wide range of impacts to global circulation and weather systems. Satellite image sequences and high resolution coupled ocean-ice-atmosphere studies have captured summer minima sea ice concentration and extent decline trends (Maslowski et al. 2012). Particularly, this decline underpins the urgency for enhanced understanding of processes controlling Arctic ice cover as shown by the 2019 summer sea ice minima in Figure 1.

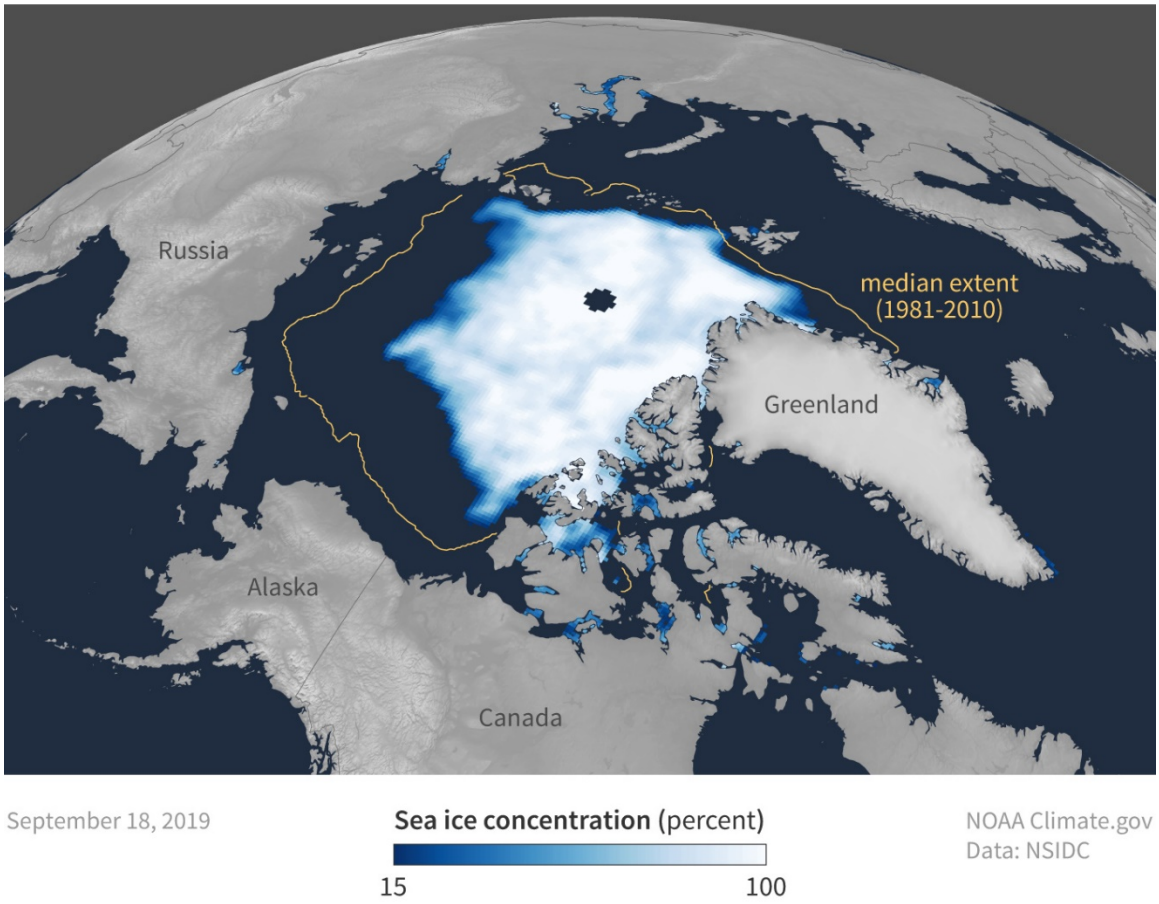

Figure 1: A Visual of 2019 Summer Minimum Ice Extent Compared with Median Extent (1981–2018). Source: NOAA NSIDC (2019).

The Arctic Ocean is the northernmost ocean sourced mainly by Atlantic water, Pacific water in the western side, sea ice melt, glacial melt, and river runoff. The Arctic contains a strong salt-stratified pycnocline that largely isolates the warmer and denser Pacific and Atlantic waters below the fresh, well-mixed, and cold surface layer.

Modeling the earth system in coupled climate models provide some predictability of these Arctic changes, but consistently overpredicts Arctic ice extent. An improved understanding of physical processes through observations, data analysis, and research with the subsequent model parameterizations will increase model accuracy.

B. ARCTIC FIELD RESEARCH MOVING TO AUTONOMOUS SYSTEMS

Surface Heat Budget of the Arctic Ocean (SHEBA) was a major field campaign in the Arctic that gathered oceanographic and atmospheric data over a year in 1997-1998 from a ship-supported drifting ice camp in the Beaufort Sea. The resulting data set from SHEBA is still used for comparison and basic understanding of the physical processes occurring in the Arctic.

While the interest in the Arctic has increased, so have the costs of being able to do large scale studies on ice flows while having continuous scientific presence at a particular ice floe. These increased costs and technology progression has led to the development and use of autonomous instruments. These scientific instruments work by sending data through satellite links to archives used for scientific research.

C. ICE AND OCEAN BOUNDARY LAYER

In order to refine the climate models sea ice extent predictions, the ice ocean boundary layer (IOBL) model physics must represent small scale processes below the model grid scale (typically 2–10 km). The small scale processes include heat exchange, wind forcing, turbulence, albedo, and solar radiation which are not captured at the grid scale of regional coupled climate models. Upper ocean turbulence distributes heat entering the ocean through solar radiation during the summer, and up from the strongly stratified pycnocline during strong wind forcing events. Turbulence and variability of the ocean and atmosphere near the IOBL impact ice through top and bottom melting. Upper ocean dynamics are influenced by wind caused drag force on the ice surface. Wind forcing and ocean currents such as the Beaufort Gyre (BG) deform the ice pack and sources of heat from the deeper ocean and strong solar summer radiative heating control ice formation.

In late summer, a marginal Ice Zone forms in the Beaufort Sea. The ice thickness reduction over the summer season has impacts on both basal melting rates and surface melting of snow and ice, and the formation of melt ponds (Gallagher et al. 2016). Basal melting is enhanced due to the ice-albedo feedback loop (AFL). This feedback loop arises from the 0.9 to 0.95 albedo (fraction of reflected solar radiation from the surface) of ice and snow, compared with the 0.2 reflectivity of open water. As open water or melt ponds

occur in the ice pack during the summer, more solar radiation can enter the ocean. This additional heat causes enhanced ice edge and basal melting, which in turn increases the amount of solar heating, resulting in a strong positive feedback (Curry et al. 1995). Ice melting was 60% attributed to the atmospheric fluxes, including the local radiation warming the upper ocean (Steele et al. 2010). A heightened polar amplification of ice top melting lead to both lower ice pack extent in the Arctic and an increased amount of bottom ice melt (Steele et al. 2010).

Solar radiation impacts the amount of heat present in the IOBL heat budget during summer months when the sun is constantly above the horizon. As the summer season progresses, there is an evolution from sea ice melt being top melt dominated to bottom melt increasing to dominance as the solar radiation inputs reduce (Steele et al. 2010). The ice provides an insulation from solar radiation as its high albedo reflects solar radiation so the more ice, the less solar radiation inputs into the Arctic Ocean.

D. COMPARING THE TRANSPOLAR DRIFT AND BEAUFORT SEA

The Marginal Ice Zone (MIZ) experiment provided an intensive summer through fall view of the evolution of the Central Beaufort Sea ice pack. Gallaher et al. (2016) showed that radiative fluxes to the ocean could be estimated through a combination of in situ shortwave radiation measurements and satellite imagery estimates of open water fraction (Gallaher et al. 2016). This study found that 1-D heat budgets closed well, suggesting a minimal lateral advection term in these budgets. Instead of the expected wave-driven Marginal Ice Zone, during 2014 the Central Beaufort formed a widespread Thermodynamic Marginal Ice Zone across much of the Canada Basin (Gallaher et al. 2016). Timmermans et al. (2018) showed that over the last three decades the Beaufort Gyre upper ocean halocline heat content has almost doubled and is linked to solar heating.

The Transpolar Drift has a more convergent ice flow along with thicker sea ice in contrast to the more divergent Beaufort Gyre. In a decadal Transpolar Drift comparison study, Stanton et al. (2012) found that Open Water Fraction (OWF) largely controlled annual integrated ice-ocean heat fluxes, while the incident solar radiation means were relatively constant year to year.

Figure 2 illustrates sources of spatial variability of both bathymetric and Arctic ocean water. Note that the ocean mixed layer (ML) which in Figure 2 is labeled the polar mixed layer, has relatively little regional variability owing to its contact with the ice cover.

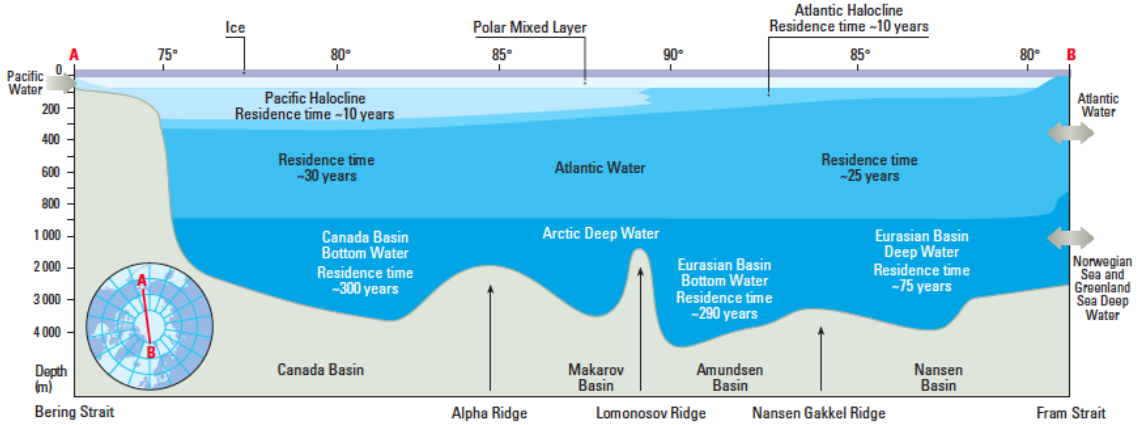

Arctic vertical cross-section showing key bathymetric and Arctic water origins over spatial scale from Alaska's Bering Strait to the Fram Strait.

Figure 2: Arctic Cross-Section from Bering Strait to Fram Strait. Source: Arctic Monitoring and Assessment Program (AMAP) (1998).

E. UPPER OCEAN AND FRESHWATER CONTENT

Gallaher et al. found that light wind conditions at the Ice Ocean Boundary Layer (IOBL) allow a fresh surface layer to form (Gallaher et al. 2016). This fresh surface layer prevents mixing of the deeper trapped upper ocean radiative heat below the pycnocline to the surface layer. Weak to moderate wind forcing allows the heat in the fresh surface layer to cause rapid basal ice melting. The late summer Beaufort Sea is characterized by high surface layer heat content and rapidly increasing open water fraction. A near surface temperature maximum (NSTM) occurs just below the fresh surface layer.

The large freshwater content of the ocean mixed layer in the Beaufort Gyre is the result of Ekman pumping from anti-cyclonic circulation along with the ocean and atmospheric dynamics making the freshwater present in the region (Proshutinsky et al. 2009). Looking at decadal observations, this study found that the freshwater characteristics

vary with the surface layer characteristics, Arctic high pressure zone location, and the force of the wind curl.

F. HEAT CONTENT

Correctly predicting heat levels in the upper ocean are key to improving the global coupled ice ocean atmospheric climate models as its proximity to the ice and potential positive feedback mechanisms have strong consequences for the concentration, age, and thickness of Arctic sea ice. While there is some heat that comes up from the strongly stratified pynocline, the focus for this study is on the upper ocean heat content which is being directly driven by solar radiation entering the ocean. Density gradients forming the strong salinity dominated pynocline, inhibit upward mixing of heat transfer and make this a small term compared with solar fluxes during the summer.

Locally absorbed solar radiation that enters the upper ocean through thin ice and open water between floes becomes the primary cause of basal ice melt (Gallaher et al. 2016). Near surface fresh layers are enhanced by melt pond drainage. These surface layers trap ocean heat due to small salinity density differences below just below the fresher (due to the ice melt water) ice ocean boundary layer preventing mixing of heat deeper into the ocean mixed layer (Gallaher et al. 2016).

Gallaher et al. 2016 found that in the marginal ice zone and ocean mixed layer (OML) "that at least 89% of total OML heating came from local radiative fluxes." This analysis also showed that across the Canada Basin there was a correlation between melt pond drainage and when the summer surface layer formed. Summer mixed layer (sML) onset increased basal ice melt due to the combination of solar radiation and turbulent mixing forced by low speed summer winds. Timmermans et al. determined that sea ice extent is sensitive to changes in ocean heat flux (2018). The heat flux along with subsequent heat content underpin the decline in sea ice extent.

G. SUMMER EVOLUTION OF THE ICE-OCEAN BOUNDARY LAYER

During the Arctic summer, near-constant sunlight produces significant solar radiation absorption in the IOBL. Melt ponds form as snow and ice melt collect in surface

pools. Gallaher et al. (2016) divided the summer evolution of the ice-ocean boundary layer into four distinct phases. In stage 1, the early summer ice-ocean conditions have a predominately ice and snow covered surface, the beginning of increased solar radiation, and very weak winter mixed layer (WML) stratification. Maximum solar radiation inputs and limited basal melt are reached in this stage. The formation of melt ponds begins to occur in depressions on the ice surface. Lowered albedo from the surface melt water intensifies melting from the solar radiation.

Mixing layer freshening and warming are the main physical processes occurring in Stage 2. The transition from Stage 1 is identified by increases in ocean mixed layer heat and decreased IOBL depth. Melt ponds increase in areal extent as the solar radiation continues. A large increase in ocean radiative fluxes to the ocean occurs due to decreased ice coverage and melt pond area and depth increases. The surface mixed layer freshens as melt pond drainage occurs, nearly concurrently across the Beaufort Sea in 2014.

The transition from Stage 2 to Stage 3 is identified by a summer mixed layer and near surface temperature maximum formation (NSTM). The NSTM is a seasonal feature created from shortwave solar radiation entering the ocean mixed layer then becoming trapped below the surface mixed layer by weak density gradients formed by ice meltwater freshening the surface layer. This heat is trapped until it is entrained upward in the early fall (Timmerman et al. 2010). During the MIZ experiment summer phase, melt pond extent decreased while the open water fraction increased from 5% to 26% in 9 days (Gallaher et al. 2016). Open water fraction increased with wind forcing having a positive wind stress curl. The summer mixed layer deepened during this stage from around 1 m to 20 m.

During the Marginal Ice Zone (MIZ) summer study, open water fraction (OWF) increased by Stage 4 and then increased to 50% by the end of the stage with some of the instruments in open water. The high open water fraction allowed increased ocean radiative heat fluxes even as incoming solar radiation reduction occurred from the shortening daylight. The ice melt rates overall were around 2 cm per day over this last stage (Gallaher et al. 2016).

H. SODA EXPERIMENT AND OBJECTIVES

A Department Research Initiative (DRI) within the Office of Naval Research funded the Stratified Ocean Dynamics in the Arctic (SODA) which is an ongoing five-year research program, with observations being made in the Canada Basin using a combination of fixed moorings, underwater gliders, satellite imagery, and ice-deployed drifting instrument systems. SODA is motivated by the observed changes in increased open water fraction and upper ocean stratification during the summer in the Beaufort Sea region. The observations are taking place in order to understand the interactions of wind forcing, ice ocean boundary layer turbulence, mixing, and ocean vertical heat transport. The primary field work occurred summer and fall 2018 with additional work taking place in the 2019 fall.. The Naval Postgraduate School research team participated in the United States Coast Guard Cutter (USCGC) Healy ice breaker SODA cruise during fall 2018, deploying three autonomous ocean flux buoys (AOFBs) on three multiyear ice floes in the Beaufort Sea with co-located Ice-Tethered Profilers deployed by Woods Hole Oceanographic Institute (WHOI). High resolution Synthetic Aperture Radar (SAR) imagery was captured throughout the experiment. Upper ocean structure measured by the AOFB's and Ice Tethered Profilers (ITPs) during SODA and other Arctic experiments form the primary data set used in this study.

I. STUDY OUTLINE

This thesis research supports several SODA experiment objectives by observing and improving the physical understanding of the Beaufort Sea upper ocean heat content changes over time. Comparisons with the Arctic regions of the Beaufort Sea and Transpolar Drift will examine upper ocean heat content and their changes over a decadal time scale. Will there be a correlation between the upper ocean heat content maximum and the ice extent or open water fraction maximum? How does the change in summer heat content over 10 years in the Beaufort compare with the 10 year change in the Transpolar? What are the magnitudes of Transpolar Drift heat content changes compared with those in the Beaufort Gyre? It is thought that heat content will increase throughout the last decade based on the declining ice minimum extent (Figure 1).

This Arctic oceanography thesis is organized as follows. Chapter II and III discusses the data sources then methods of the observational instrument setup, governing equations, and then how the analysis calculations were made. Chapter IV presents the quantitative results and analysis between differences and similarities in time and space. Chapter V focuses on key findings and recommendations for future research.

THIS PAGE INTENTIONALLY LEFT BLANK

II. OBSERVATIONS AND DATA SOURCES

The Arctic environment is both expensive to reach and challenging to instrument. This is where the autonomous instruments designed for the Arctic are beneficial by feeding scientific data back to research labs year around from multiple locations. The Autonomous Ocean Flux Buoys (AOFBs) and ITPs (Ice Tethered Profiler) have been productive instrument observers in some of the harshest environments of the world, with a primary focus on Arctic Oceanography and more specifically, the ice ocean boundary layer dynamics. Comprehensive data sets gathered by these systems allow for both spatial and temporal views when looking at a changing Arctic Ice Extent and the physical process differences between the Beaufort Gyre and the Transpolar Drift.

Autonomous instruments were deployed as part of a range of funded research projects performed by the Ocean Turbulence group at the Naval Postgraduate School (NPS) and the WHOI ITP group over the last two decades. Thousands of profiles of upper ocean profiles will be utilized from the Woods Hole Oceanographic Institute (WHOI) Ice Tethered Profilers (ITP) and Naval Postgraduate School (NPS) Autonomous Ocean Flux Buoys (AOFB). Data sets will be selected for the period 2009 through 2019. Since the AOFB's and ITPs are deployed on ice floes that drift in response to a wide range of wind events, they do not always stay within the study area. Also, instrument lifespan depends on the buoys on surviving frequent ice deformation events of the ice pack.

These substantial data sets have been screened to meet the requirements of providing high resolution Temperature and Salinity (T and S) profile time series spanning the ocean mixed layer to 100 m, well into the strongly salinity-stratified pycnoline.

A. WHOI ITP AND NPS AOFB

The Ice Tethered Profiler (ITP) observation data were downloaded from Woods Hole Oceanographic Institute public archive, and more information can be found on their website (ITP 2019). Basically the ITP is crawler device that moves a Sea Bird Electronics Conductivity-Temperature-Depth (CTD) instrument up and down a 800 m weighted wire. The CTD profiler package moves up and down the plastic-coated steel tether wire at a

speed of 25 cm/s sampling at 1 Hz giving around a 0.25 m vertical sample spacing. The profiler is connected to a surface buoy deployed through the ice (Figure 3).

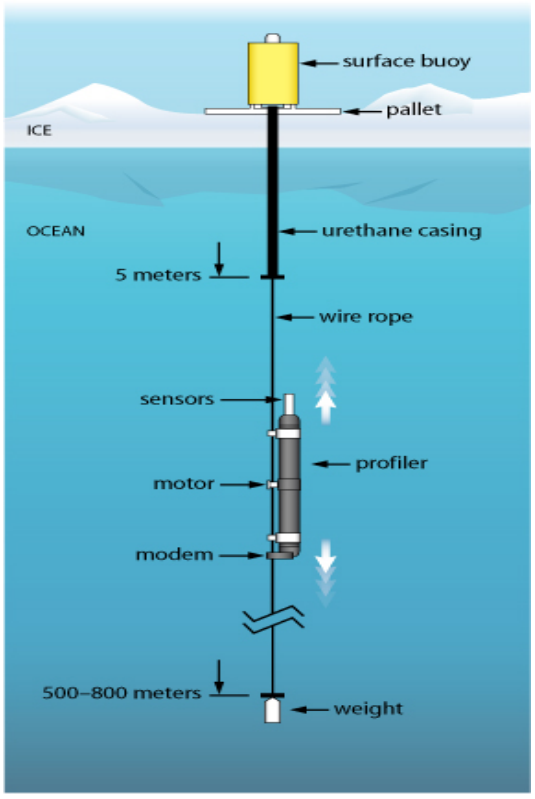

Figure 3: ITP Schematic. Source: ITP (2019).

Data is averaged to 2 m depth bins before transmission by an inductive modem to a surface unit that then sends the data via an Iridium modem link to WHOI. The vertical sampling operates up to a depth of 800 m, with programmable vertical sampling depths and time intervals. The ITP upper ocean observational data include time, salinity, temperature, location, and depth (Toole et al. 2010). In this study, the focus will be on the upper 100 m of ocean data spanning the mixed layer and upper part of the pycnocline. The CTD data sampling begins at 10 m and became the main data source, but additional near surface data was added into the temperature, salinity, time, and depth matrix to create the final matrix archive for each ITP. The need for the additional data closer to the surface was driven by the focus of this study being the upper ocean. One additional source of data

present on some of the WHOI ITPs were the WHOI ITP microcat Temperature/Conductivity (T/C) data at a depth of 6 m (6 decibars).

Another data source was T/C data from the Naval Postgraduate School Autonomous Ocean Flux Buoy (AOFB) custom-built ocean flux package at shallower depths of 4 m. The AOFB ocean temperature timeseries were taken every 2 hours as part of the eddy correlation flux measurement time series sampling (AOFB 2019). The AOFB schematic shown as Figure 4 works similar to the ITP for sending oceanographic data via Iridium satellite.

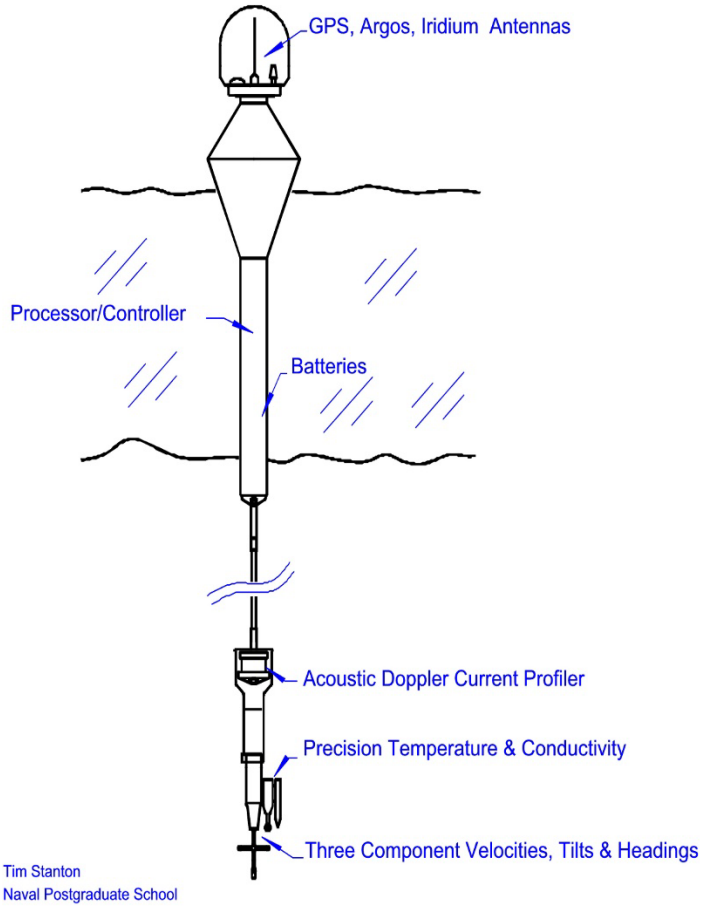

Figure 4: AOFB Schematic. Source: AOFB (2019).

The dates for available data were those in Table 1 organized by instrument type, instrument number, and dates they were actively recording ocean data. The final archived matrix of salinity, temperature, and pressure (depth) incorporated data from all available sources. The AOFB data was interpolated to be at the same time interval as the main ITP data matrix archive. The upper most data in the profile matrix archive was then extrapolated up to the surface in the 2 m bins by exploiting that upper ocean mixing takes place in the late summer.

Table 1: Available ITP and AOFB Data Including Time and Deployment Location. Adapted from Camarato (2019).

AOFB #	AOFB Active Dates	ITP #	ITP Active Dates	Region
10	9/4/2006-1/5/2007	6	9/4/2006-10/11/2009	BG
11	4/28/2007-12/18/2007	7	4/28/2007-2/7/2008	TPD, NPEO
12	8/14/2007-9/17/2008	13	8/13/2007-9/7/2008	BG
13	8/16/2007-10/15/2008	18	8/16/2007-10/21/2008	BG
15	4/8/2008-12/30/2008	19	4/7/2008-11/22/2008	TPD, NPEO
17	8/4/2008-1/10/2011	23	8/5/2008-9/3/2011	BG
21	10/8/2010-8/18/2012	43	10/7/2010-2/10/2011	BG
22	10/5/2010-2/26/2011	42	10/4/2010-7/31/2011	BG
24	8/27/2012-9/24/2013	65	8/27/2012-9/10/2013	BG
25	8/6/2011-9/21/2012	54	8/6/2011-?	BG
28	4/17/2013-6/14/2013	61	4/10/2013-11/24/2013	TPD, NPEO
29	8/12/2014-10/5/2015	86	8/15/2014-8/26/2015	BG
30	8/25/2013-8/30/2013	79	3/19/2014-9/30/2014	BG
31	4/11/2014-11/29/2014	76	4/11/2014-12/9/2014	NPEO

AOFB #	AOFB Active Dates	ITP #	ITP Active Dates	Region
32	3/17/2014-5/28/2016	78	3/11/2014-8/6/2014	BG
33	3/10/2014-8/23/2014	77	3/9/2014-10/2/2014	BG
35	4/10/2015-1/3/2016	93	9/22/2015-1/2/2017	NPEO
36	9/13/2015-2/21/2016	92	9/12/2015-2/22/2016	Siberian Sea
37	10/2/2015-9/24/2016	89*	10/2/2015-9/6/2016	BG
38	4/11/2017-?	95	4/11/2017-1/6/2018	TPD, NPEO
40*	10/1/2018-active	103*	10/1/2018-active	BG
41*	10/3/2018-active	104*	10/3/2018-active	BG
42*	10/6/2018-active	105*	10/6/2018-active	BG

BG=Beaufort Gyre TPD=Transpolar Drift, NPEO=North Pole Environmental Observatory, and *=currently active.

B. OBSERVATION AREAS

The observational AOFB tracks can be seen overlaid on a generalized Arctic map (Figure 5). The key on the right hand side corresponds buoy number to color on the map. The map shows the Beaufort Gyre tracks in the upper left hand side and the Transpolar Drift starting at the center by the North Pole.

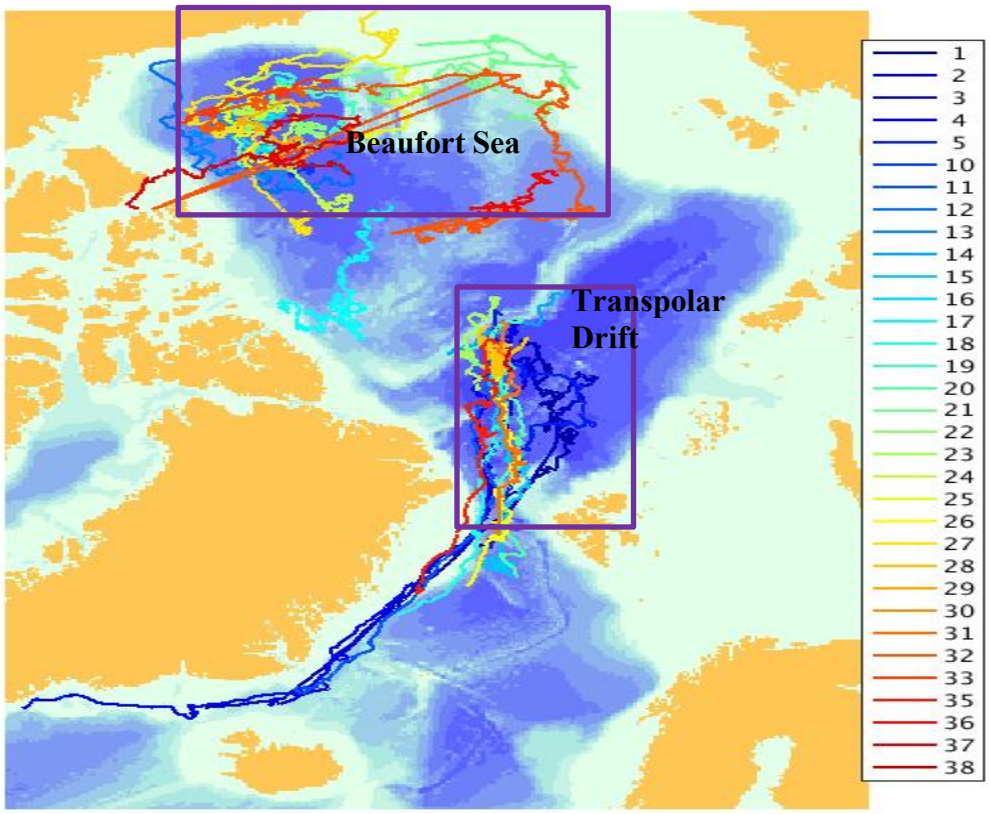

Figure 5: AOFB Arctic Track Map by AOFB Number Often Collocated with ITPs. Source: AOFB (2019).

1. Marginal Ice Zone Experiment (MIZ)

MIZ consisted of an Arctic ice deployments joint effort by University of Washington Applied Physics Laboratory, Woods Hole Oceanographic Institute, Naval Postgraduate School, and others funded through ONR (Lee et al., 2012). Both AOFBs numbered 32 and 33 collocated with ITPs 77 and 78 were deployed during this larger experiment to understand the edge of the Beaufort Gyre were the summer conditions are resulting in a reduced decadal ice extent (Lee et al., 2019).

2. Stratified Ocean Dynamics of the Arctic (SODA)

SODA experiment 2018 and 2019 consisted of a joint effort by U.S. Coast Guard Healy, University of Washington Applied Physics Laboratory, Woods Hole

Oceanographic Institute, Naval Postgraduate School, and others funded through ONR (SODA 2016). The experiment deployment included 3 collocated ITPs and AOFBs in the Beaufort Gyre in 2018. Additional instrumentation was put out in fall of 2019, but not incorporated into this study.

3. North Pole Environmental Observatory

The most consistent data source for the Transpolar Drift were AOFB and ITP deployments at the North Pole Environmental Observatory (NPEO) funded by the National Science Foundation (NSF). NPEO remains an ongoing international scientific community effort to gather Arctic information at the North Pole region (NPEO 2019).

Additional data in the archive consists of other experiments and instrument deployments when opportunities were available.

THIS PAGE INTENTIONALLY LEFT BLANK

III. METHODS

A. CREATING THE TEMPERATURE, SALINITY, AND DEPTH MATRIX ARCHIVE

The data from all the different sources described in Chapter II were combined to create depth / time matrices of temperature, salinity and density. Temperature/Salinity (T/S) data from different sources were matched to the ITP profile sampling times and inserted into the profile matrices. Linear interpolation from AOFB times was used to match the ITP data times. “NaN” (not a number) values were assigned to depth entries with no observational data available. Most of the data gaps occurred near the surface in high currents when the profiler had difficulty reaching its 10 m nominal start depth. Another place in the profiles where “NaN” were common was near the bottom of the profiles, but these areas were excluded in this study by focusing only on the upper 100 m. Salinity spikes occasionally occur in CTD data if contaminants enter the pumped conductivity cell, or if there is a mismatch between the temperature and conductivity sensor time responses due to the CT sensor pump being partially blocked. These bad points have been edited out or in the case of ITP 19 the whole time series has been eliminated. The problem with a difference between the up and down profiles differing significantly due to a T/C pump flow problem is shown in Figure 6. In a correct scenario, with the pump working correctly, up and down density anomaly profiles would be tracking in agreement with each other.

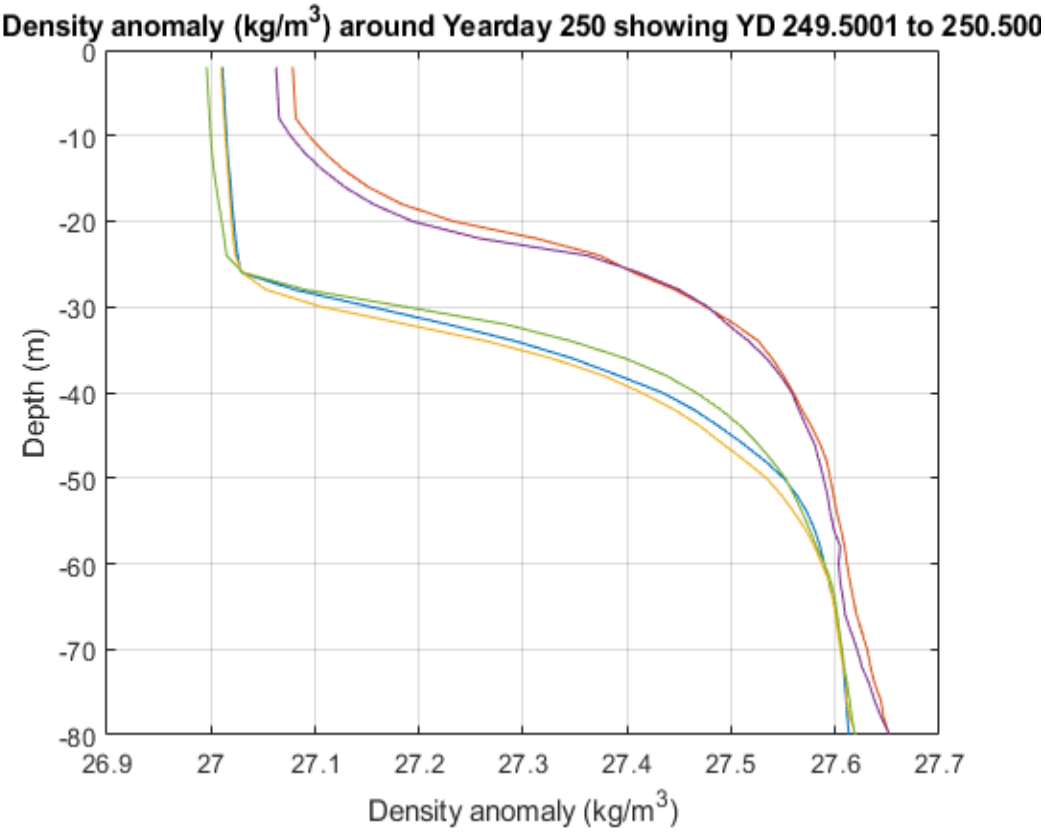

Figure 6: AOFB Arctic Track Map by AOFB Number Often Collocated with ITPs. Source: AOFB (2019).

Another quality control aspect is determining if the profiles resolve most of the ocean mixed layer. The profiles have CTD observations near the surface, but not all the way to the surface. The mixed layer allows for the extrapolation to the surface, but the degree each mixed layer was resolved is not uniform across all the profiles. For the rest of this study, the names "profiles" or "observations" will refer to the T/S matrices of edited and interpolated arrays in the archive and not in their original raw format of measurement. A manual inspection process of the full profiles identified a few other anomalies visually, and these data were then excluded from the analysis.

Automated screening methods developed in MATLAB were applied to each profile to determine its validity leaving only the good profiles for that particular ITP. One such screening technique was to flag all of the profiles with more than 10 "NaN" values in the upper 200 m and then either remove them or interpolate them based on the before and after

data points available. The ITP profiles without a pressure value equal to or less than 10 decibars, equivalent to 10 m were eliminated.

The time series plots shown in Figure 7 provide an example of what the profiles' depth to top bin looked like before removing the bad data. For yearday 200 to 280 there are some measurements not taken until the depth of over 100 m shown by the y axis. The density anomaly time series on top showed the missing data holes indicating instrumentation errors during those time periods and the needed removal.

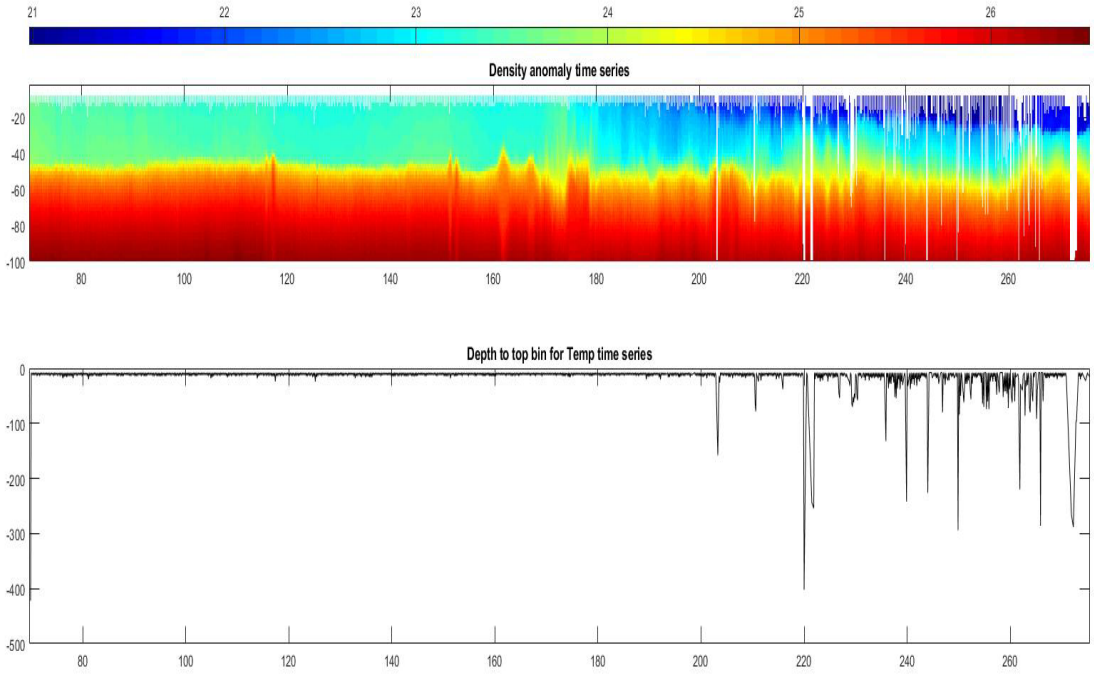

Figure 7: One ITP Number Density Anomaly Time Series and Depth to First Recorded Data for the ITP Profiles

After the process of eliminating profiles from the archive that contained bad data through both the manual and automatic methods, the archived data was extrapolated up to the surface. For many cases the top data bin was 6 m, and these T,S and density anomaly values were filled in to the surface. An archive matrix of temperature and salinity values completed to the surface was necessary to integrate for heat content.

B. IDENTIFYING THE UPPER OCEAN INTEGRATION BOUNDARIES

The density gradients below the ocean mixed layer prevent ocean properties from efficiently mixing vertically. A density isopycnal has been chosen to define the integration limit for upper ocean heat content. In this process, for each profile the interpolated depth of the isopycnal value was calculated, then used for the heat content lower integration limit.

Density is primarily controlled by salinity in for the T/S conditions found in the Arctic Ocean, which is why a salinity time series was graphed to show the depth of the isopycnal used. The time series shown in Figure 8 indicates that the depth to the lower integration limit is tracking with the halocline in the salinity profile as indicated by the blue line representing the lower integration limit density isopycnal. The density isopycnal was chosen based on a 0.06 kgm^{-3} density increase from the upper most surface density value for each profile in the time series for all of the Transpolar Drift cases.

The Beaufort Sea cases required a different upper ocean integration boundary process as the data is not well resolved at the surface due to the development of the seasonal, shallow, fresh layer in the late Summer. The density material surface was based on the winter mixed layer halocline surface occurring around 35 to 40 m. The density anomaly, sigma-theta, value at the surface for yearday 140 before the summer changes plus a 1.0 kgm^{-3} density increase defined the lower integration boundary.

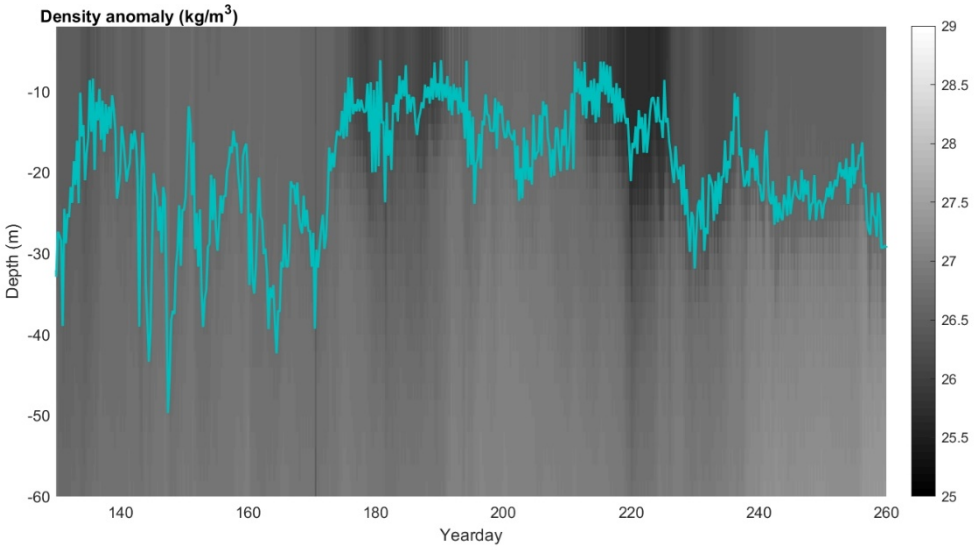

Figure 8: Density Anomaly Time Series and the Blue Line Is Depth of Isopycnal Defining Heat Content Integration Lower Limit

This method for determining the mixed layer depth (MLD) assumed that the MLD occurred between the surface and 100 m depth. The method also assumes that the largest vertical gradient known as the halocline will be only slightly below the base of the mixed layer depth for each profile.

Surface layer heat content is a key focus of this study, providing a depth integration of the amount of energy in this layer with units of megajoules per meter squared (MJm^{-2}). The temperature is expressed as the departure from the in situ freezing point of seawater. Heat content (HC) is evaluated with the equation:

$$HC = \rho Cp \int_{Z2}^{Z1} (T - Tfp)dz \qquad (1)$$

where z1 is the surface data depth, while z2 is the depth of the isopycnal equal to the surface value + 0.06 Kg m^{-3}, dz represents the discreet depth increment of 2 m while density (ρ) is the in situ density. Specific Heat (Cp) = 3850 Jkg^{-1} C^{-1}. The Freezing Point (T_{fp}) is calculated from the in situ salinity and pressure.

C. ICE SPEED

Ice speed is calculated through the use of the ITP GPS data being converted into the distance divided by the time in matlab. The ice speed will be used to describe the ice and ocean conditions at the summer ice minima extent of September 15.

Ice speed (IS) is evaluated with the equation:

$$IS = \sqrt{(x2 - x1)^2 + (y2 - y1)^2} \,/\, (\sec 2 - \sec 1) \tag{2}$$

where x2 is the easting distance of 2nd GPS point, while x1 is the easting distance at 1st GPS point, y2 and y1 follow this same pattern. Sec2 represents the time at GPS point 2 in seconds and sec1 is point 1 in seconds, resulting in m s^{-1} ice speed units.

D. AMSR DATA

Advanced Microwave Scanning Radiometer-Earth Observing System (AMSR) data was used from the National Snow and Ice Data Center (NSIDC 2019). The AMSR measures brightness which for the polar region is used for estimates of the amount of snow and ice cover compared to the amount of open water. The AMSR data used in this study has already had the open water and sea ice estimated along the AOFB and ITP drift tracks. A time series for the open water fraction and spring through fall yeardays enabled a view of when the Fall refreeze of the Arctic ice began for each case of interest.

E. ANALYSIS

The vertical integrals from the various final archived profiles were computed by year for the Beaufort Sea and Transpolar Drift regions. The Beaufort Gyre had more observations compared with the Transpolar Drift. However, the Beaufort Gyre observations were not as consistent both in start time and location of instrument deployment. The challenge became selection of the right season, right year, and right location for comparison over the last decade to see long term trends in heat content. The time of year criteria selected to address the summer season questions in this study are from yearday 130 (May 10th) to yearday 260 (September 17), as this is close to the NOAA-

reported sea ice minima of September 16 based on the last 10 years (U.S. National Ice Center 2018).

THIS PAGE INTENTIONALLY LEFT BLANK

IV. RESULTS AND DISCUSSION

A. BEAUFORT SEA AND TRANSPOLAR DRIFT TIME SERIES

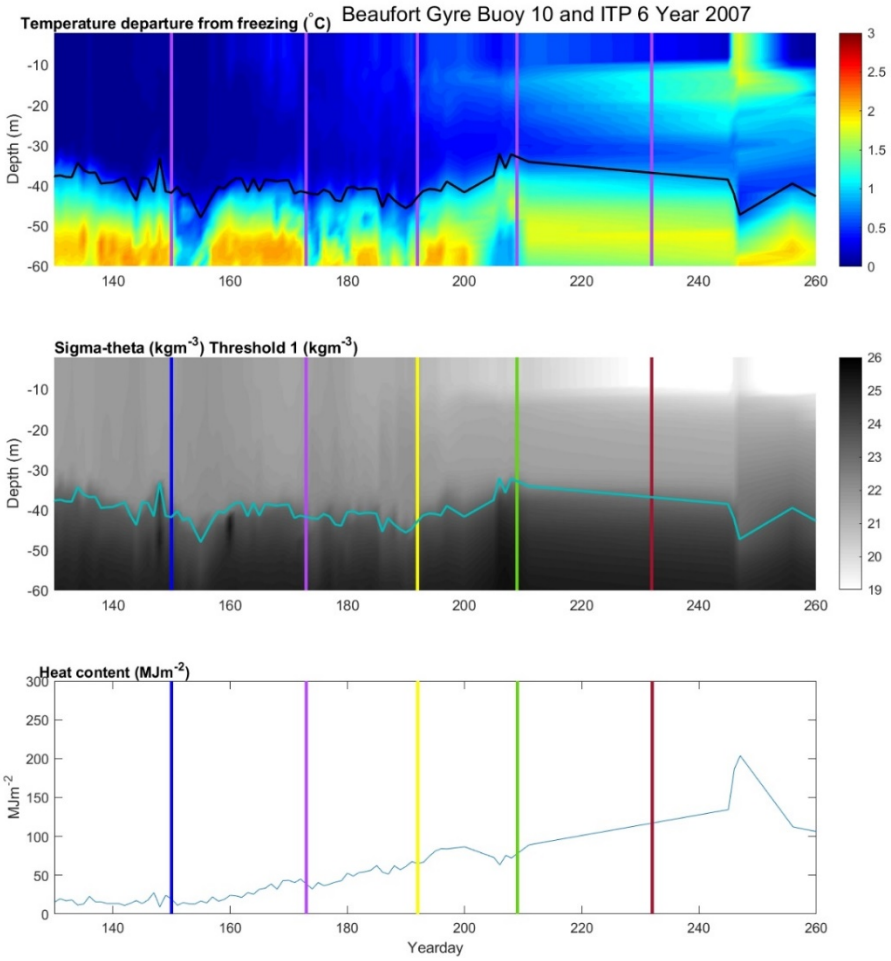

A. Top Panel: Temperature departure from freezing (TDF) by depth time series with yearday 140 reference surface SIGMA plus threshold as black line B. Middle Panel: Sigma-theta by depth time series with yearday 140 reference surface SIGMA plus threshold as blue line Surface C. Bottom Panel: Heat content time series. The three panel figures show the start of Gallaher et al.'s stage 1 indicated by the blue line, start of stage 2 with the purple line, start of stage 3 with the yellow line, start of stage 4 with the green line, and end of stage 4 the red line (2016).

Figure 9: Beaufort Sea Year 2007 ITP 6

The Beaufort Sea 2007 timeseries (Figure 9A) displays the temperature departure from freezing occurring from 0 to 1.2 degrees Celsius with the exception of the heat below the winter mixed layer occurring at a depth of 40 m below the ice surface. There is another more notable exception outside of the 0 to 1.2 degrees Celsius occurring at around yearday 250 from the surface to a depth of 25 m. It was initially suspected that this was an instrumentation error, but upon further analyses there was no recognizable error in the data set or data processing. The same late summer heat content and high value for late summer temperature departure from freezing was also found for the Beaufort Sea Summer 2008 ITP 18 case (Figure 10A). The reasoning behind the suspicion is that the physical process occurring in the summer near the surface is that any additional heat is used to melt the ice instead of heating the upper ocean. The ice acts as a regulator of the heat near the surface. When local ice concentration is low, we can expect more dramatic heat of the upper ocean as seen in the two records. The near surface temperature maximum (NSTM) begins to occur around yearday 190 at a depth of 15 m. It is indicated by the amount of heat below the near surface freshwater layer. Data resolution above 10 m was not available in much of the data archive matrix. The sigma-theta, insitu density anomaly, (Figure 9B) displays the material surface of the integration lower boundary being followed by the yearday 140 reference surface SIGMA plus threshold depth value. The greatest heat content occurs in the later summer after Gallaher et al.'s stage 4 (Figure 9C). The maximum value is 203.9 MJm^{-2} occurred at yearday 247, September 4, 2007.

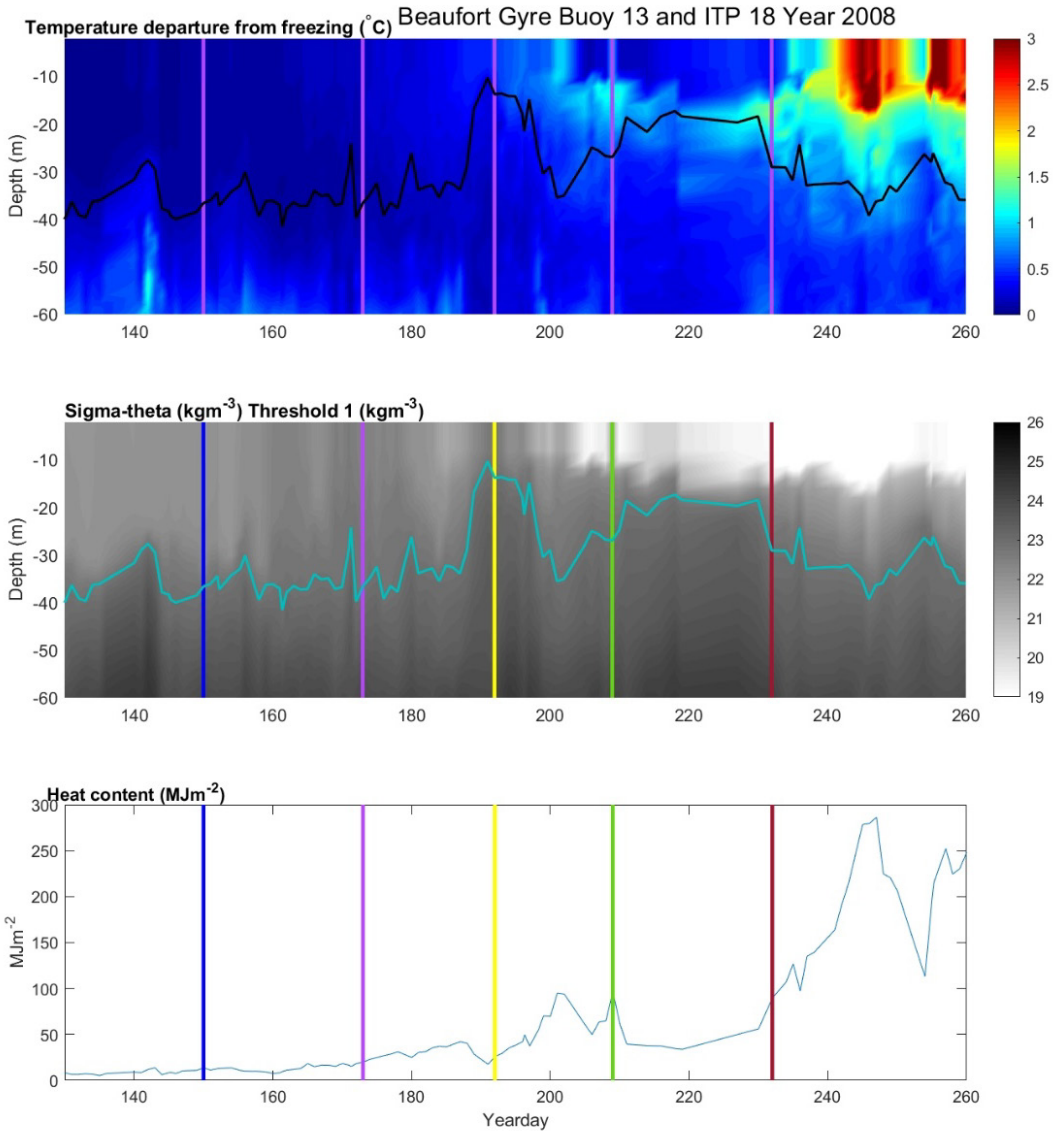

A. Top Panel: Temperature departure from freezing by depth time series with yearday 140 reference surface SIGMA plus threshold as black line B. Middle Panel: Sigma-theta by depth time series with yearday 140 reference surface SIGMA plus threshold as blue line Surface C. Bottom Panel: Heat content time series.

Figure 10: Beaufort Sea Year 2008 ITP 18

Like Beaufort Sea 2007 example, late-summer, near-surface heat content is present in Beaufort Sea 2008 (Figure 10A), It appears briefly at yearday 200, but consistently appears after yearday 230, reaching from the surface to 30 m depth. The integration lower boundary shown on the sigma-theta plot is slightly above the values in Beaufort Sea 2007 (Figure 9B), but still in an expected range from 40 m to 15 m and sigma-theta values from around 19 kgm^{-3} to near 24 kgm^{-3}. The below-surface, fresher layer is seen around yearday 190 from the surface to 12 m depth. This layer arises from sea ice melt in the summer. The heat content (Figure 10C) increases significantly in the late summer from yearday 230, (August 17, 2008, as it is a leapyear) to yearday 260 (September 16, 2008). The greatest heat content occurs in the later summer after Gallaher et al.'s stage 4 (Figure 10C). The maximum value is 286.4 MJm^{-2}, occurring at yearday 247 (September 3, 2008). The yearday of the maximum heat content is the same as in Beaufort Sea 2007 (Figure 9C).

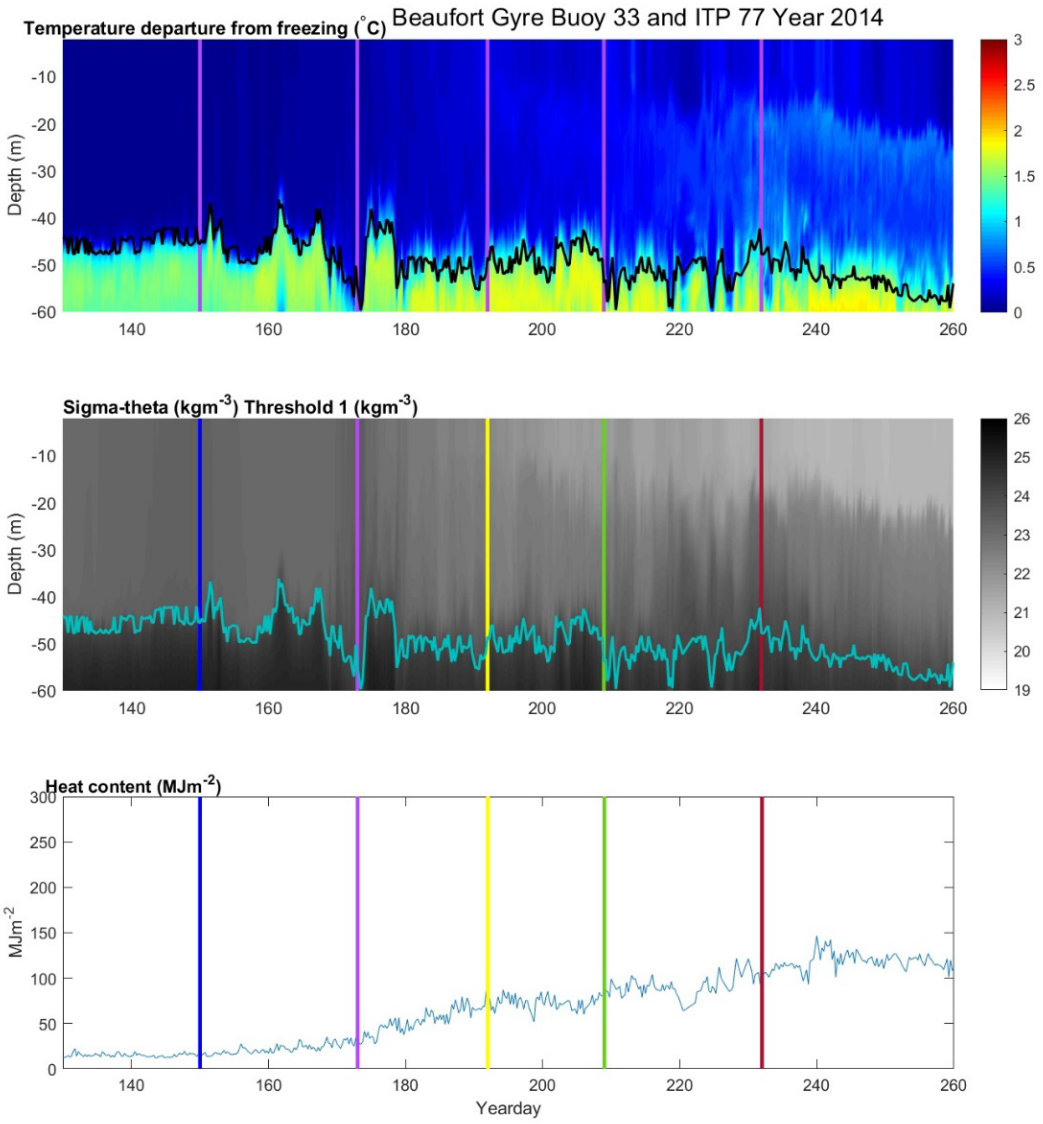

A. Top Panel: Temperature departure from freezing by depth time series with yearday 140 reference surface sigma-theta plus threshold as black line B. Middle Panel: Sigma-theta by depth time series with yearday 140 reference surface sigma-theta plus threshold as blue line Surface C. Bottom Panel: Heat content time series.

Figure 11: Beaufort Sea Year 2014 ITP 77

The Beaufort Sea 2014 data in this study told a different story than the Beaufort Sea 2007 and 2008 late summer heat content. The amount of heat contained in the Beaufort Sea 2014 mixed layer (Figure 11A) is dwarfed by that in Figures 9A and 10A for the late summer. The sigma-theta material surface lower integration boundary stayed at depth of around 45 m over the displayed timeseries (Figure 11B) staying at the WML isopycnal material surface. The maximum heat content value of 146.5 MJm^{-2} occurred at yearday 240 (August 28, 2014). The yearday of the maximum value occurs a week sooner than in 2007 and 2008 for the Beaufort Sea. The slow heat content increase over the time series is more gradual than that occurring in the 2007 and 2008 Beaufort Sea cases, where there is a steeper slope at the end of summer.

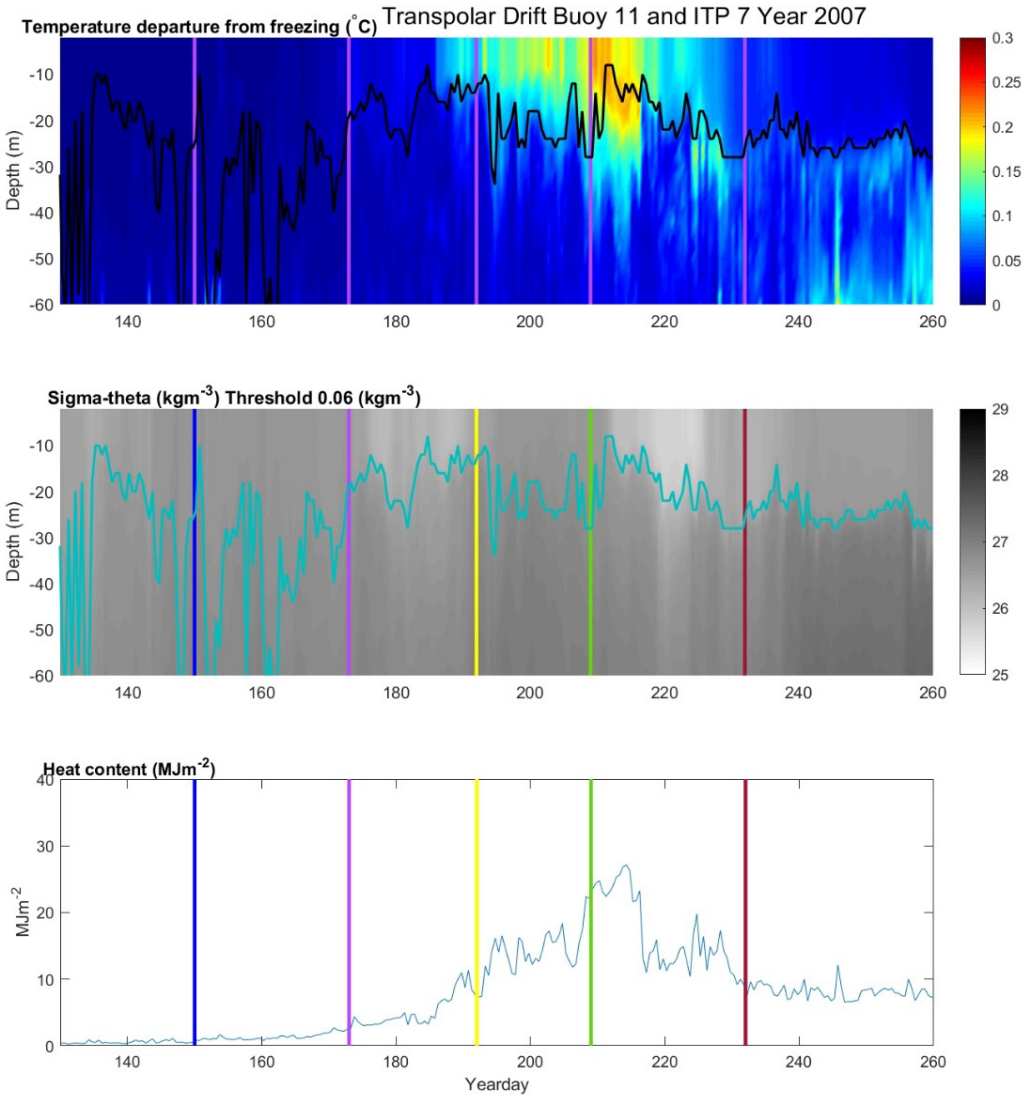

A. Top Panel: Temperature departure from freezing by depth time series. The black line represents the depth of sigma-theta 0.06 Kg m^{-3} greater than the surface value. B. Middle Panel: Sigma-theta by depth time series and the blue line represents the depth of sigma-theta 0.06 Kg m^{-3} greater than the surface value. C. Bottom Panel: Heat content time series.

Figure 12: Transpolar Drift Year 2007 ITP 7

The scale ranges for the Transpolar Drift (TPD) for all three plots in the panel than in the Beaufort Sea. The sigma-theta is around 5 kgm^{-3} greater with a range from 25 to 29 indicating denser water (Figure 12B). The Transpolar Drift heat content (Figure 12C) reaches a maximum value of 27.15 MJm^{-2} at yearday 214. The value is 120 MJm^{-2} less than all of the Beaufort Sea cases. However, the heat content maximum occurs earlier in the late summer than for the Beaufort cases. The Transpolar Drift records feature a highly variable integration depth lower boundary until the summer mixed layer has formed around yearday 170 (Figure 12A/B). This is due to the TPD not having as strongly stratified of a pycnocline as the Beaufort Sea. The heat content increase starts at the time of formation of the summer mixed layer (Figure 12C).

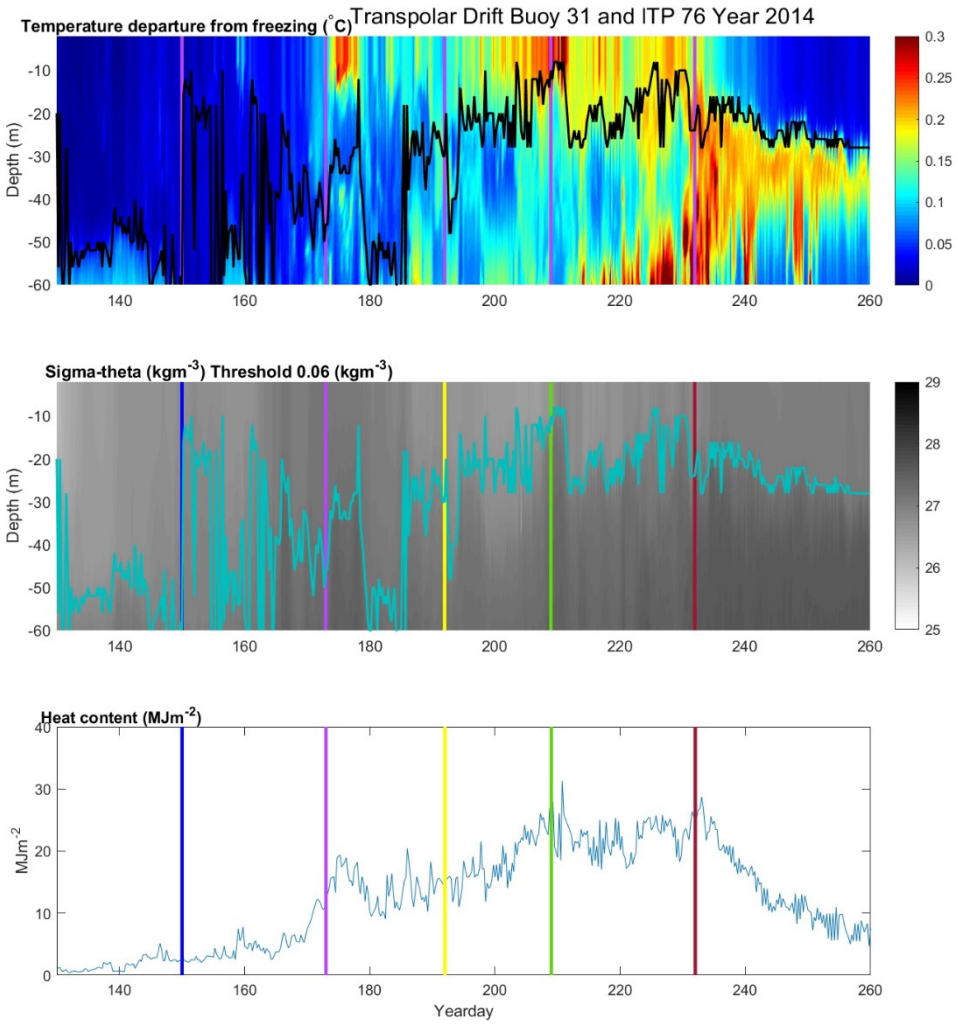

A. Top Panel: Temperature departure from freezing by depth time series. The black line represents the depth of sigma-theta 0.06 Kg m^{-3} greater than the surface value. B. Middle Panel: Sigma-theta by depth time series and the blue line represents the depth of sigma-theta 0.06 Kg m^{-3} greater than the surface value. C. Bottom Panel: Heat content time series.

Figure 13: Transpolar Drift Year 2014 ITP 7

For the Transpolar Drift 2014, the isopyncal material surface follows above the near surface temperature maximum as indicated at yearday 225 (Figure 13A). The sigma-theta is around 5 kgm^{-3} greater with a range from 25 to 29 indicating denser water. The heat content (Figure 13C) reaches a maximum value of 31.32 MJm^{-2} at yearday 210.8. The

maximum heat content value is 4 MJm^{-2} more than in the 2007 case and occurs 4 days earlier. The heat content increase also begins to occur sooner around yearday 170, whereas in the 2007 case it begins around 190. This Transpolar Drift case is similar to the TPD 2007 case as it also has the heat content maximum occurring earlier in the late summer than for the Beaufort cases by around 30 days.

B. BEAUFORT SEA DRIFT TRAJECTORIES

The Beaufort Sea location in the Arctic Ocean is shown in the methods section (Figure 5). The individual collocated ITPs and AOFBs display the location over the time series of the Beaufort Gyre as well as the specific colors for the yeardays of interest. The 2007 case (Figure 14) starts in the central Canada Basin and drifts to the northwestern edge of the Canada Nasin. The 2014 Beaufort Sea case (Figure 15) moves westward over the deeper, southern portion part of the Canadian Basin, north of Alaska.

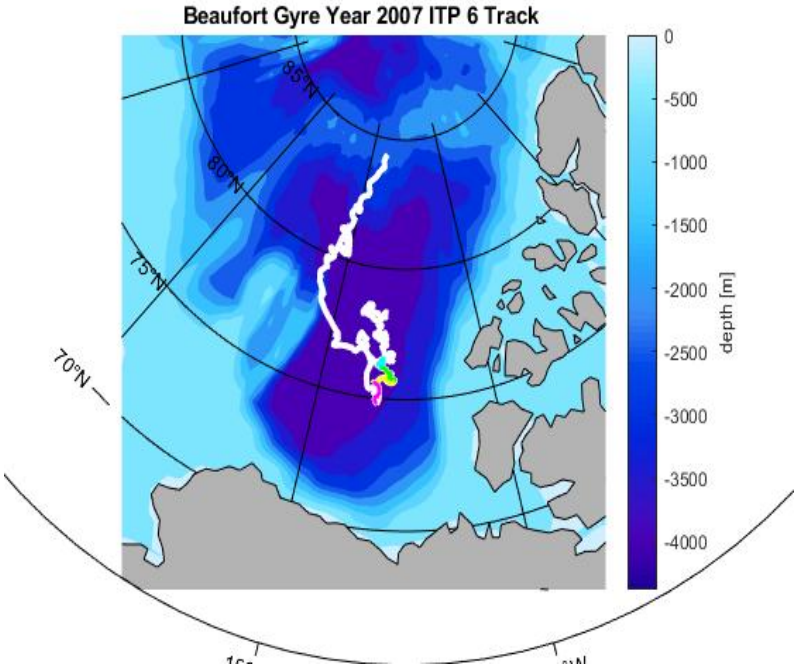

The beginning of Gallaher et al.'s stage 1 is indicated by the light blue line segment, stage 2 with the green line segment, stage 3 with the yellow line segment, and stage 4 is with the bright pink line segment (2016).

Figure 14: Beaufort Sea Year 2007 ITP #6 Map Track.

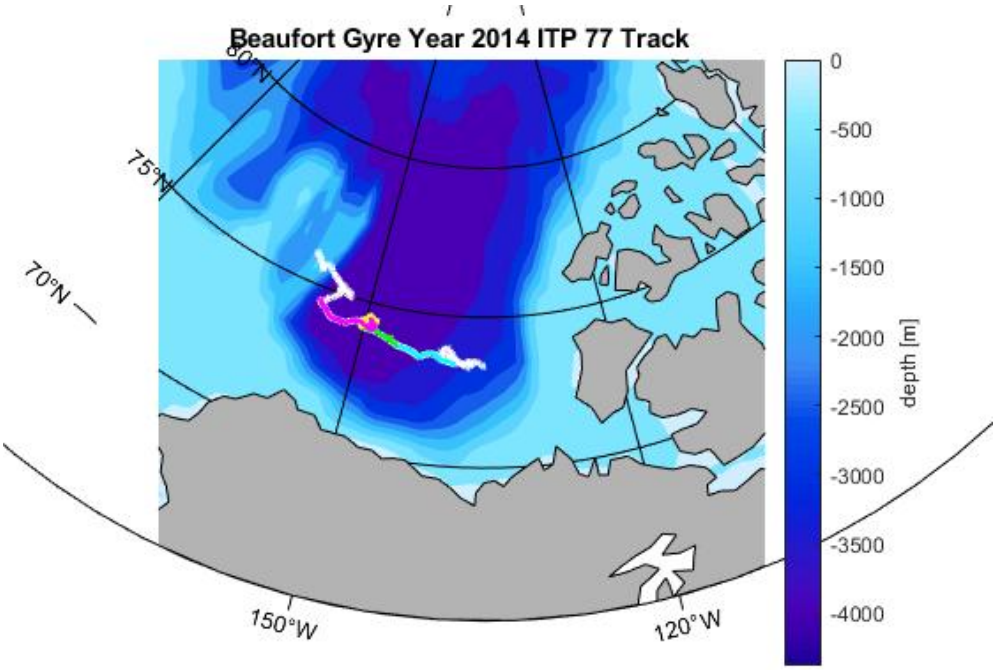

Figure 15: Beaufort Sea Year 2014 ITP #77 Map Track

C. TRANSPOLAR DRIFT TRAJECTORIES

The Transpolar Drift location in the Arctic Ocean is shown in Figure 5. The individual collocated ITPs and AOFBs display the location over the time series of the Transpolar Drift as well as the specific colors for the yeardays of interest. The 2007 (Figure 16) and 2014 (Figure 17) cases cover close to the same time of year and drift trajectory path from near the North Pole out through the Fram Straight. Beaufort Sea ITP's drift trajectories have more temporal and spatial variability in the 3 cases.

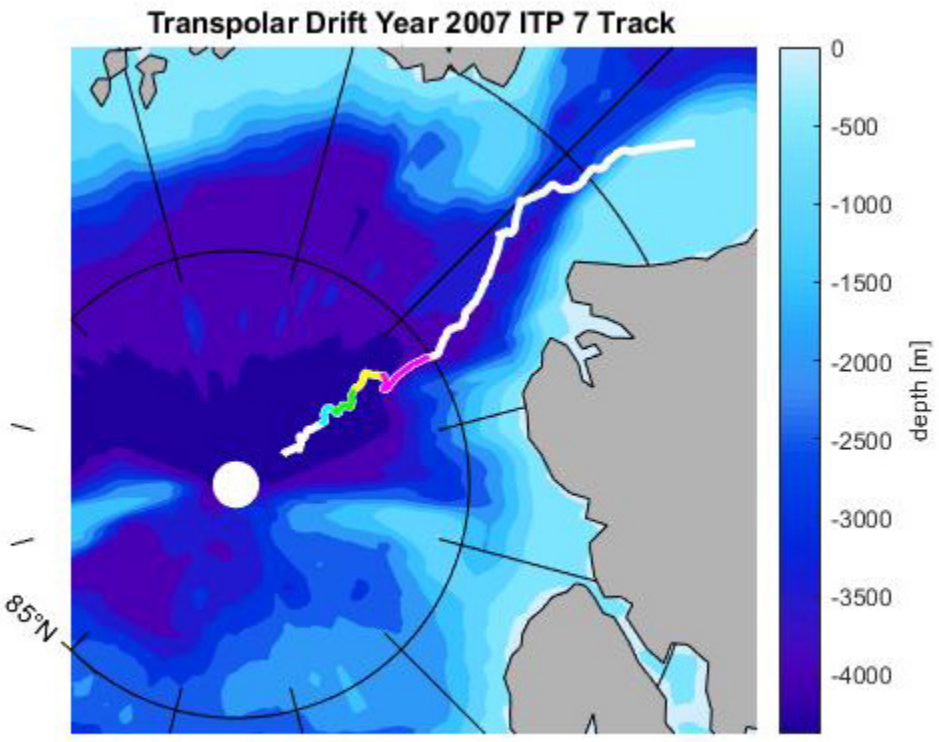

The beginning of Gallaher et al.'s stage 1 is indicated by the light blue line segment, stage 2 with the green line segment, stage 3 with the yellow line segment, and stage 4 is with the bright pink line segment (2016).

Figure 16: Transpolar Drift Year 2007 ITP #7 Map Track

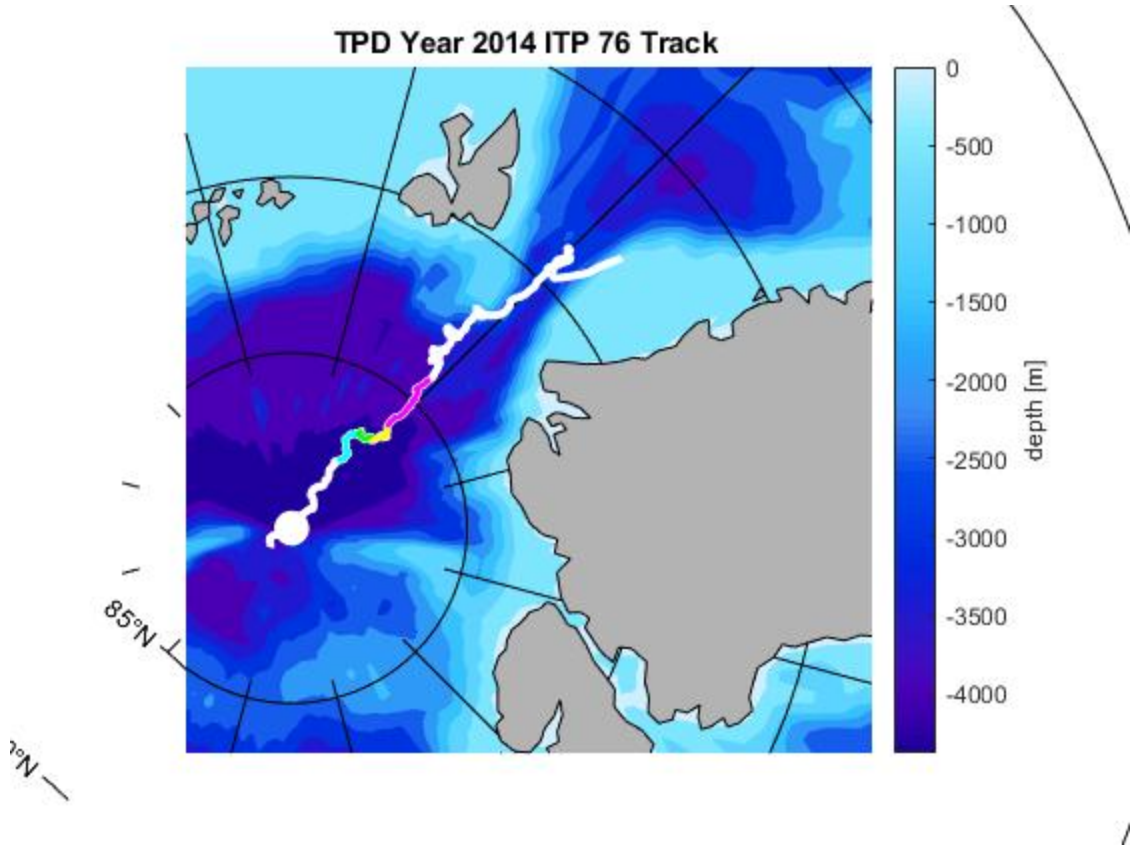

The ITP positions are displayed on an Arctic bathymetric map in white and takes place in the Transpolar Drift into the Fram Strait with a variable depth from 4000 m towards 1000 m in the strait.

Figure 17: Transpolar Drift Year 2014 ITP #76 Map Track

D. HEAT CONTENT AND ICE SPEED SUMMARIES

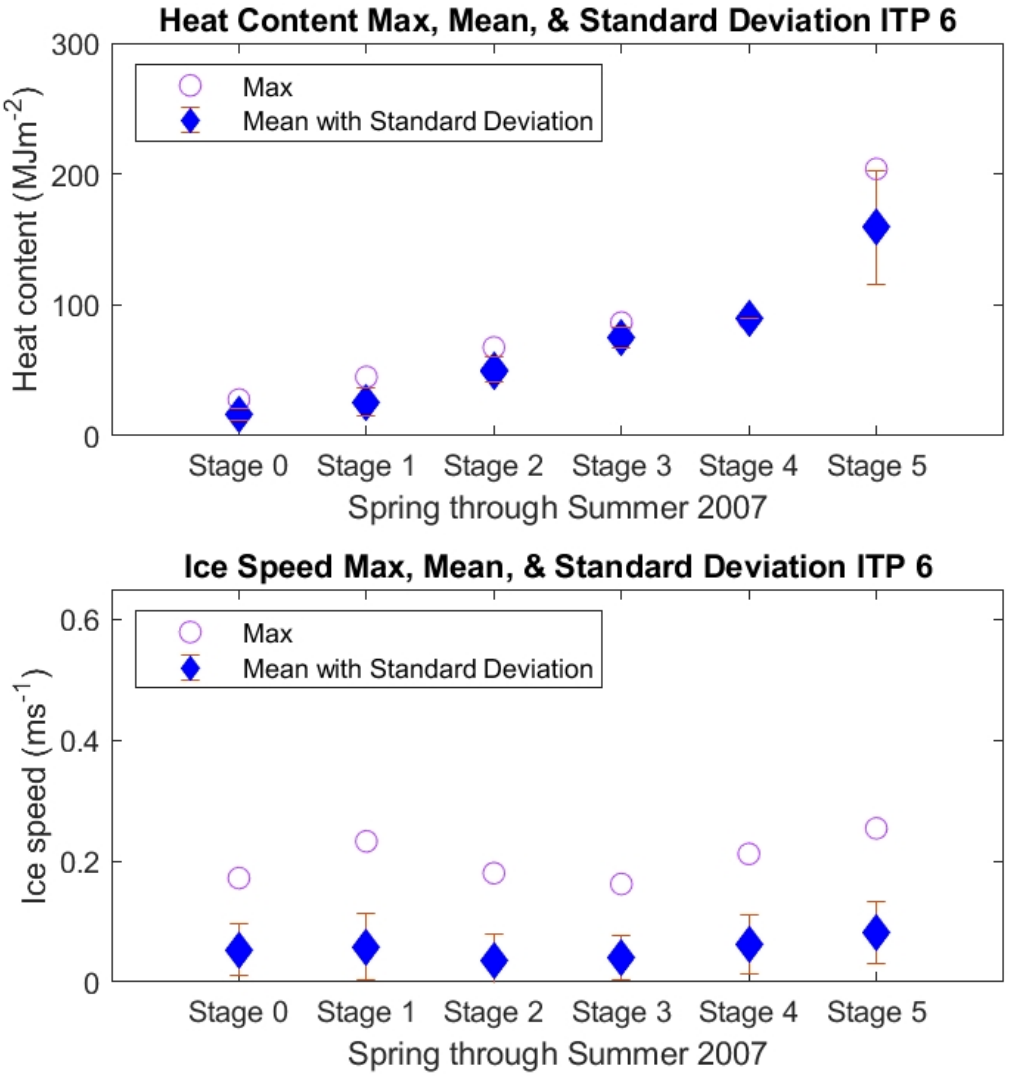

Stage 0 yeardays 130-150, Stage 1 yeardays 150-173, Stage 2 yeardays 172-192, Stage 3 yeardays 192-209, Stage 4 yeardays 209-232, Stage 5 yeardays 232-260. A. Heat Content Max, Mean, and Standard Deviation B. Ice Speed Max, Mean, and Standard Deviation

Figure 18: Beaufort Sea 2007 ITP #6 Heat Content and Ice Speed over 6 Stages from Spring through Summer 2007

Beaufort Sea 2007 (Figure 18A) heat content shows a consistent increase throughout the stages to a maximum value of near 200 MJm^{-2}. The standard deviation of this value increases in the late summer, when the upper ocean temperature and salinity data were challenging to resolve. The ice speed mean and max over the stages do not display a significant trend and have low ice speed values averaging less than 0.15 ms^{-1}.

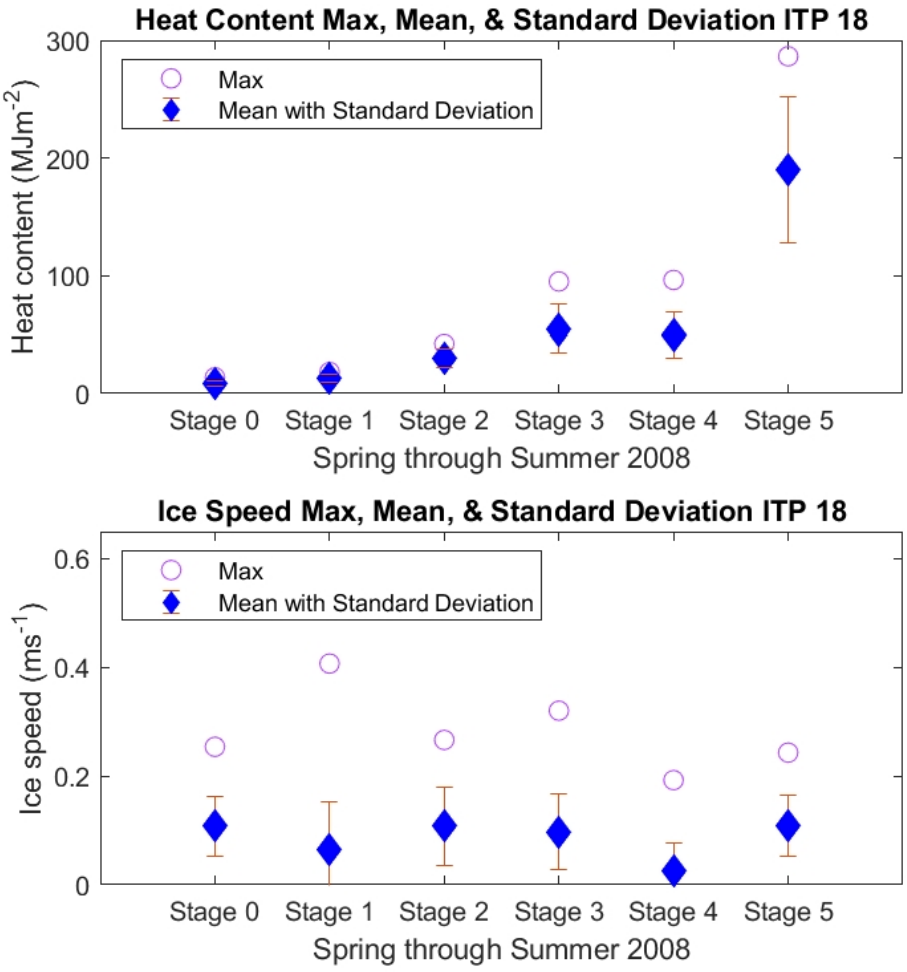

A. Heat Content Max, Mean, and Standard Deviation B. Ice Speed Max, Mean, and Standard Deviation

Figure 19: Beaufort Sea 2008 ITP #18 Heat Content and Ice Speed over 6 Stages from Spring through Summer 2008

Beaufort Sea 2008 (Figure 19A) heat content displays a consistent increase throughout the stages and ice speeds stay under 0.5 ms^{-1} for each stage (Figure 19B). The heat content shows an inconsistent slope increase throughout the stages, though stage 3 and 4 have roughly the same mean value (Figure 19A). The stage 5 heat content has a large maximum and wide standard deviation line indicating the uncertainty in the mean value (Figure 19A).

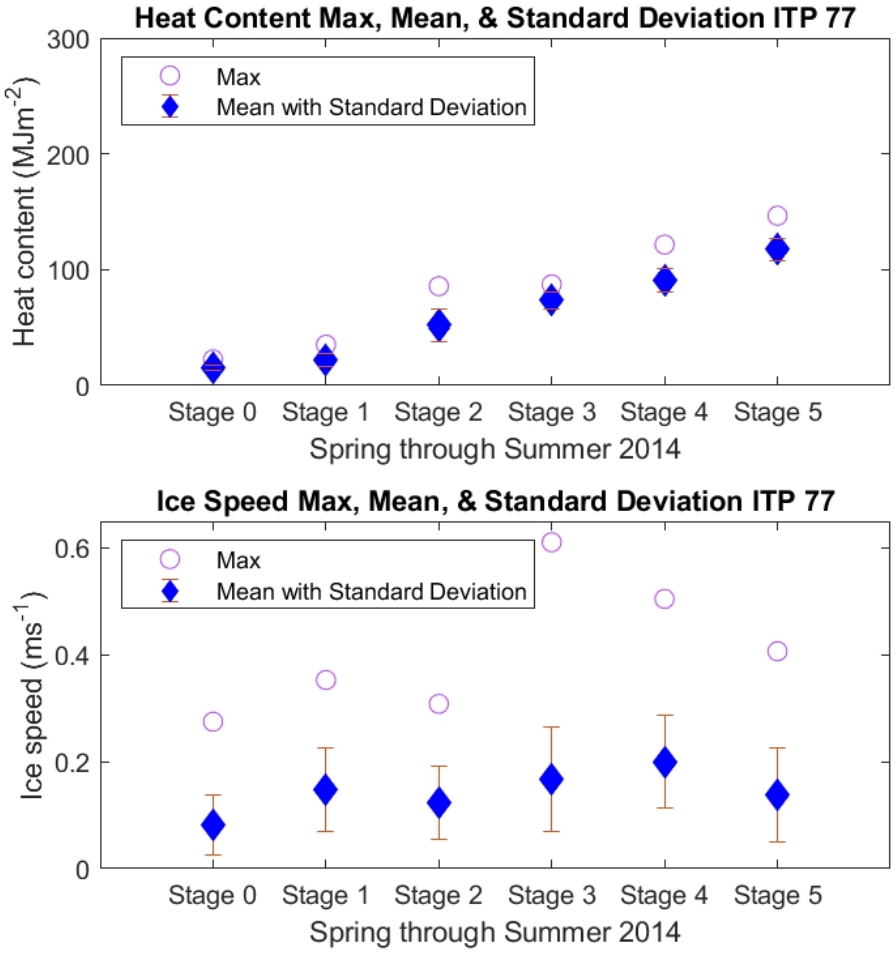

A. Heat Content Max, Mean, and Standard Deviation B. Ice Speed Max, Mean, and Standard Deviation

Figure 20: Beaufort Sea 2014 ITP #77 Heat Content and Ice Speed over 6 Stages from Spring through Summer 2014

Beaufort Sea 2014 (Figure 20A) heat content shows a consistent, linear-slope increase throughout the stages and ice speeds varies significantly for each stage when focusing on the maximum ice speed values (Figure 20B). The heat content standard deviation is significantly less in Stage 5 for this Beaufort Sea Case than the 2007 and 2008 cases, indicating increased certainty of the estimates. Wind forcing, expressed by the ice drift speed (Figure 20B), influenced heat content of the surface layer by transporting heat to the base of the ice and by entraining heat from below the shallow summer mixed layer into the upper layer. Stage 3 and 4 maximum ice speed values of 0.6 ms^{-1} and 0.5 ms^{-1} suggest turbulent transports were large during this periods. The forcing causes ocean turbulence and heat fluxes within and below the ice ocean boundary layer. The entrained heat became available for use in the process of melting ice into the late Summer and early Fall.

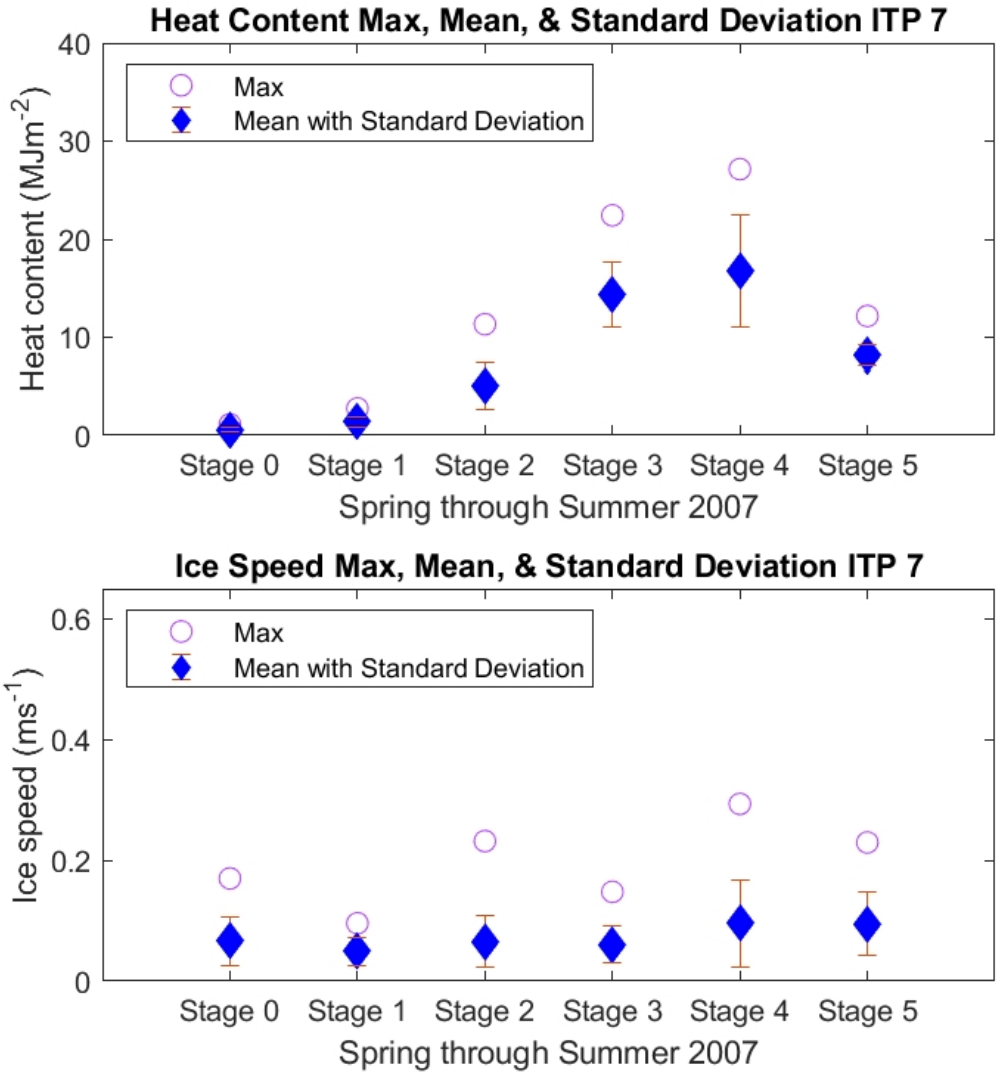

A. Heat Content Max, Mean, and Standard Deviation B. Ice Speed Max, Mean, and Standard Deviation

Figure 21: Transpolar Drift 2007 ITP #7 Heat Content and Ice Speed over 6 Stages from Spring through Summer 2007.

Transpolar Drift 2007 (Figure 21A) heat content shows a consistent linear slope increase throughout the stages 0 to 4 with a sharp decline at stage 5 and ice speeds stay under 0.5 ms^{-1} for each stage (Figure 21B). The standard deviation is significantly less in Stage 5 for this Transpolar Drift 2007 case than the Beaufort Sea 2007 case. The Transpolar

Drift heat content maximum is occurring in Stage 4 instead of the Stage 5 max that occurs in the Beaufort Sea.

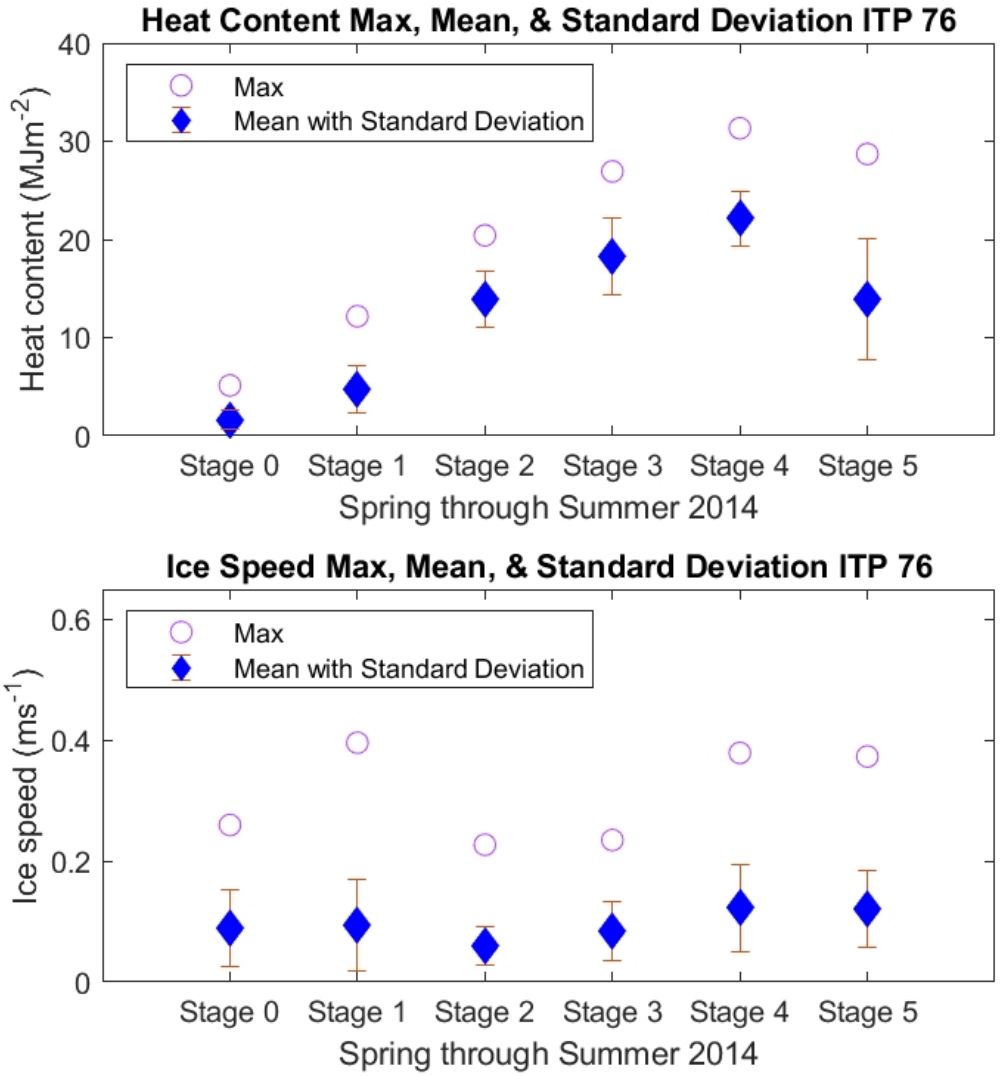

A. Heat Content Max, Mean, and Standard Deviation B. Ice Speed Max, Mean, and Standard Deviation

Figure 22: Transpolar Drift 2014 ITP #77 Heat Content and Ice Speed over 6 Stages from Spring through Summer 2014

Transpolar Drift 2014 (Figure 22A) heat content shows a consistent linear slope increase throughout the stages 0 to 4 with slight decline in value at stage 5 and mean ice speeds less than 0.2 ms^{-1} for each stage (Figure 22B). The ice speeds increase after Stage 3. The standard deviation is more in Stage 5 for this Transpolar Drift 2014 case than the Transpolar Drift 2007 case. The Transpolar Drift 2014 heat content maximum is occurring in Stage 4 instead of the Stage 5 that happens in the Beaufort Sea. This is consistent with the Transpolar Drift 2007 case (Figure 22A).

E. OPEN WATER FRACTION AMSR DATA

The Beaufort Sea 2007 (Figure 23) and 2014 (Figure 24) cases display that over the last decade there has been a delay in the beginning of the refreeze. This finding is explored further in terms of how the factors of heat content, wind speed, and open water fraction influence ice melt and early Fall refreeze. The 2007 case for yearday 200 has the same fraction of ice coverage at 0.5 as the 2014 Beaufort Sea case, but the 2014 case achieves full melt out at yearday 243 where the 2007 case lowest value is 0.3 with the refreeze beginning soon after. The 2014 case shows that the refreeze begins around yearday 260 which is a couple of weeks later than yearday 245 in the 2007 Beaufort Sea case (Figure 23).

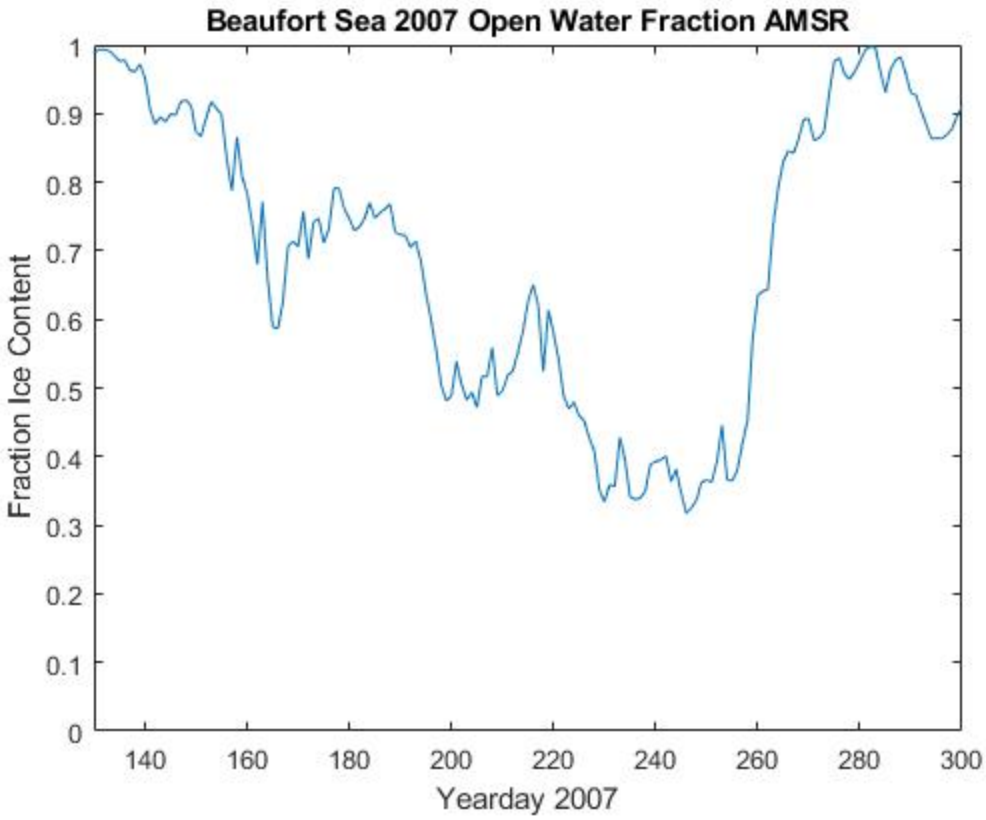

Figure 23: Beaufort Sea 2007 Open Water Fraction AMSR from Yearday 130 (May 10) to Yearday 300 (October 27)

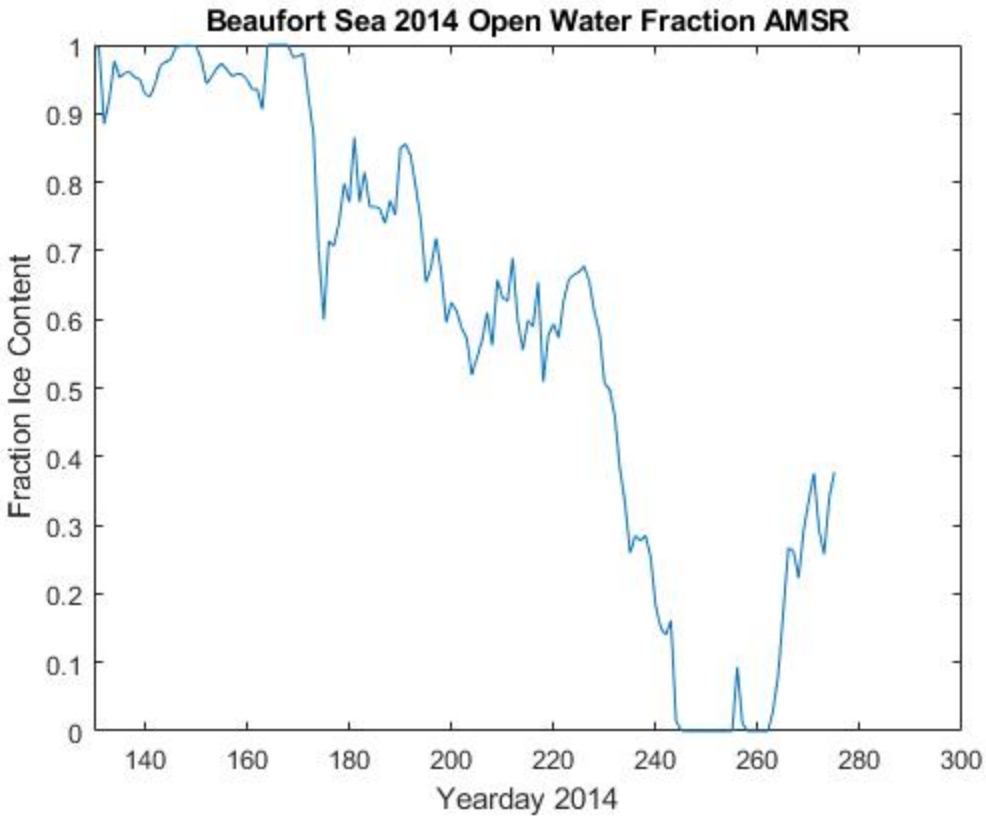

Figure 24: Beaufort Sea 2007 Open Water Fraction AMSR from Yearday 130 (May 10) to Yearday 300 (October 27)

The Transpolar Drift 2007 (Figure 25) and 2014 (Figure 26) cases display that over the time period between the two cases there has been a delay in the beginning of the refreeze. The change shown by the minimum fraction ice cover yearday 230 (Figure 25) to yearday 260 (Figure 26), with corresponding fraction ice cover minimum values of 0.65 and 0.55. The Transpolar 2014 case (Figure 26) refreeze yearday of around 260 also occurs for both the 2007 and 2014 Beaufort Sea (Figures 23 and 24).

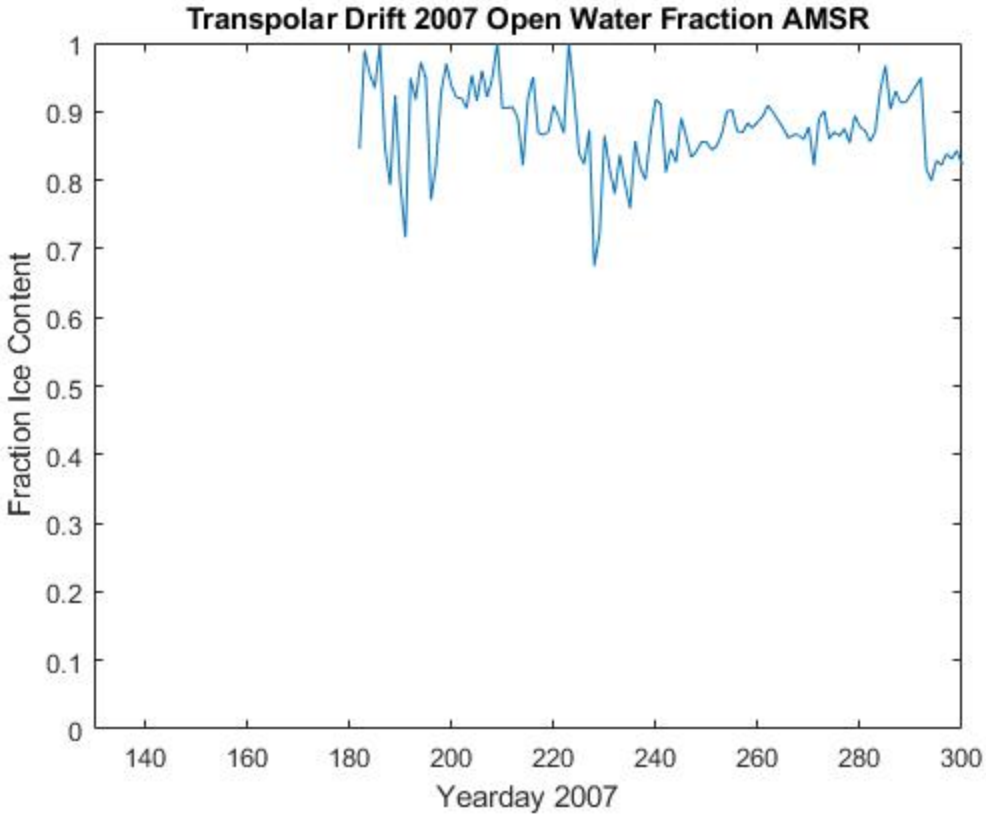

Figure 25: Beaufort Sea 2007 Open Water Fraction AMSR from Yearday 130 (May 10) to Yearday 300 (October 27)

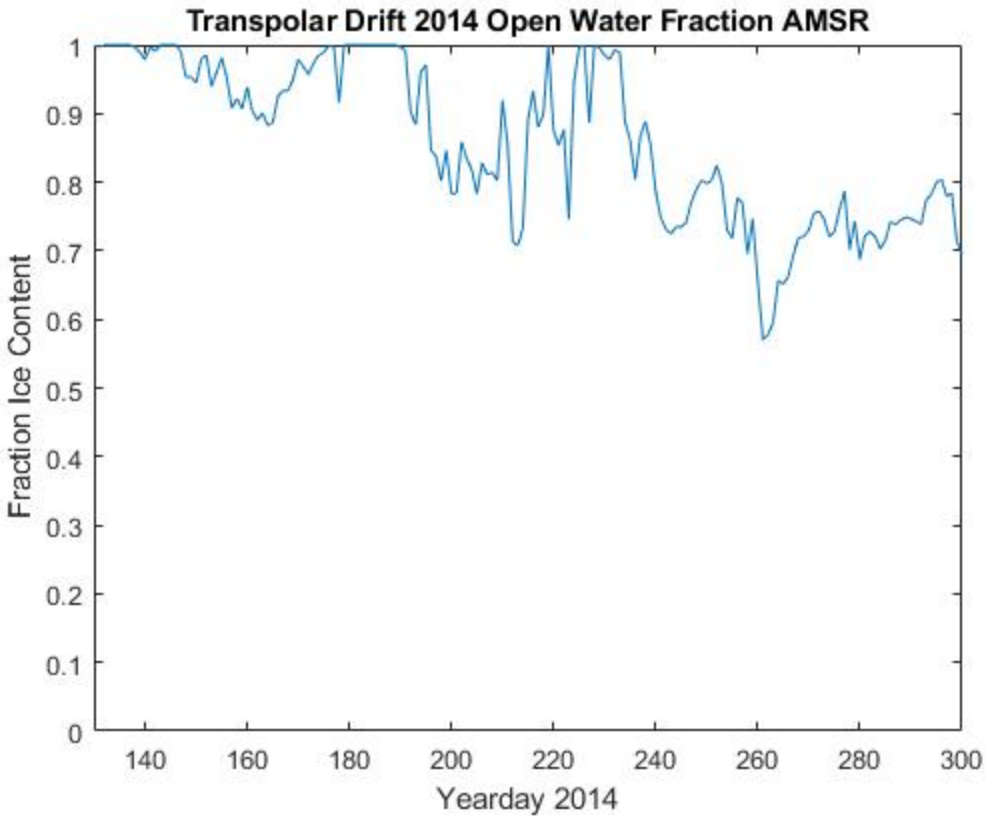

Figure 26: Beaufort Sea 2007 Open Water Fraction AMSR from Yearday 130 (May 10) to Yearday 300 (October 27)

F. COMPARISON BETWEEN BEAUFORT SEA AND TRANSPOLAR DRIFT

The ability to have a solid comparison between the two regions is hindered by the differences in the controlling factors. The Beaufort Sea is controlled by amount of heat content and Transpolar Drift is primarily controlled by local ocean structure that has density gradients extending to near the ice interface. Both of these factors affect the heat content calculation. It was known that these differences were present, but their impacts on the results were not fully appreciated until the analysis was completed. The higher heat content appeared in the Beaufort Sea and the greater density took place in the Transpolar Drift.

G. BEAUFORT SEA HEAT CONTENT, ICE SPEED, AND OPEN WATER FRACTION RELATIONSHIP

The ice speed increases in the Beaufort 2014 case as compared to the 2007 and 2008 cases create ocean turbulence from wind forcing. This wind forcing probably entrained heat from below summer mixed layer, accelerating ice melt out. In both cases, Beaufort Sea late summer heat content delays fall Arctic ice refreeze (Figures 23 and 24), which has a large impact in the region over a multi decadal scale (Figure 1).

The turbulence mixes the near surface temperature maximum in the late summer up to the surface overcoming the density gradient in the fresh surface layer to melt ice and maintain a close to 0 TDF for the Beaufort 2014 cases. The 2007 and 2008 cases were able to form a more significant and persistent late summer near surface temperature maximum (Figures 11 and 12) as those cases did not experience ice speeds larger than 0.35 ms^{-1} for stages 3 to 5 (Figures 18 and 19). In comparison the Beaufort Sea 2014 case had maximum wind speeds of 0.65 ms^{-1} . The timing of these larger wind speeds (Figure 20) coincided with the yeardays of fraction ice cover decline from 200 to 240 (Figure 24) as these yeardays start in stage 3, cover all of stage 4, and stop the beginning of stage 5. The 2007 and 2008 cases did not have as big of ice melt out as the heat maintained trapped below a surface fresher ocean layer and this near surface thin layer was not well resolved in the data used for this study.

H. DATA LIMITATIONS

A challenge, in addition to the extreme Arctic conditions with the process of acquiring proper equipment, is that the data is sparse. The data set was limited to what equipment was working especially with the salinity sensor. AOFBs and ITP locations were dependent on the speed and locations of the drifting ice floes so temporal and regional changes occurred in the dataset. ITPs do not resolve near-surface features in the ocean, this is especially difficult during the summer season when the mixed layer is shallow and when a seasonal freshwater layer occurs at the ice ocean boundary layer. There may be other factors influencing the data for this study such as eddies, advective heat, instrumentation, or instrument errors that were not identified.

I. HYPOTHESIS

The hypothesis that heat content increase is delaying freeze up conditions into the fall, as shown with the Beaufort Sea heat content and AMSR open water fraction data, is supported for these examples from the Beaufort Sea and the Transpolar Drift. However, the Beaufort Sea heat content increases expected over the last decade did not happen in the cases for this study. The relationship is more complicated, affected by the strength of wind forced mixing in the ocean and the details of air-ice-ocean interaction.

J. GENERAL SUMMARY

The temperature and salinity upper ocean profile observations from ITPs and AOFBs enabled the upper ocean heat content integrations from selected years and two Arctic regions over the last decade. There were limitations to the findings on the Transpolar Drift data, as it was found to be controlled more by local ocean density gradient structure than by surface ocean processes occurring in this region. The Transpolar Drift was found to have a heat content increase of 4 MJm^{-2} and the maximum heat content occurring 4 days sooner in 2014 than 2007. The Beaufort Sea showed that there has been a5 day delay in the ice refreeze period from 2007 to 2014 with evidence from the open water fraction AMSR data. The method of calculating heat content based on isopycnal depth has some limitations, as an isopycnal does not always represent well the base of the mixed layer.

K. FUTURE RESEARCH

The Naval Postgraduate School Multidisciplinary drifting Observatory for the Study of Arctic Climate (MOSAiC) research team deployed AOFBs with an upper carriage that will be able to be adjusted upward on a mechanical track in the summer season to near the surface to capture this layer. This data will also increase availability of data in the Central Arctic Ocean. Another Masters graduate student will be continuing to use these various tools and techniques to process SODA experiment data from 2018 and 2019. They will then develop a 1-D local heat budget at the IOBL.

LIST OF REFERENCES

AOFB, 2019: Autonomous Ocean Flux Buoy (AOFB) program. http://www.oc.nps.edu/~stanton/fluxbuoy/index.html (accessed 5 April, 2019).

Camarato, A., 2019: Thesis proposal, California State University Moss Landing Marine Labs, Moss Landing, CA.

Curry, J. A., J. L. Schramm, and E. E. Ebert, 1995: Sea ice-albedo climate feedback mechanism. *J. Clim*ate., **8,** 240–247, https://doi.org/10.1175/1520-0442(1995)008<0240:SIACFM>2.0.CO;2.

Gallaher, S. G., T. P. Stanton, W. J. Shaw, S. T. Cole, J. M. Toole, J. P. Wilkinson, T. Maksym, and B. Hwang, 2016: Evolution of a Canada Basin ice-ocean boundary layer and mixed layer across a developing thermodynamically forced marginal ice zone. *J. Geophys. Res. Ocean*., **121**, 6223–6250, https://doi.org/10.1002/2016JC011778.

ITP, 2019: Ice Tethered Profiler (ITP) program. https://www.whoi.edu/website/itp/overview (accessed 16 July, 2019).

Maslowski, W., J. C. Kinney, M. Higgins, and A. Roberts, 2012: The future of Arctic sea ice. *Annual Review of Earth and Planetary Sciences*, **40**, 625-654, https://doi.org/10.1146/annurev-earth-042711-105345.

NSIDC, 2019: AMSR-E instrument description. https://nsidc.org/data/amsre/amsre-instrument (Accessed November 9, 2019).

Proshutinsky, A., and Coauthors, 2009: Beaufort Gyre freshwater reservoir: State and variability from observations. *J. Geophys*. Res., **114**, 1–25, https://doi.org/10.1029/2008jc005104.

Stanton, T. P., W. J. Shaw, and J. K. Hutchings, 2012: Observational study of relationships between incoming radiation, open water fraction, and ocean-to-ice heat flux in the Transpolar Drift: 2002-2010. *J. Geophys*. Res. Ocean., **117**, 2002–2010, https://doi.org/10.1029/2011JC007871.

Steele, M., J. Zhang, and W. Ermold, 2010: Mechanisms of summertime upper Arctic Ocean warming and the effect on sea ice melt. *J. Geophys. Res. Ocean*., **115**, 1–12, https://doi.org/10.1029/2009JC005849.

Task Force Climate Change, Chief of Naval Operations 2014: The United States Navy Arctic roadmap for 2014 to 2030. Washington, DC. https://apps.dtic.mil/dtic/tr/fulltext/u2/a595557.pdf.

Task Force Climate Change, Oceanographer of the Navy, 2009: Navy Arctic roadmap. Washington, DC.

Task Force Climate Change, Oceanographer of the Navy, 2009: Navy climate change roadmap. Washington, DC.

Timmermans, M. L., J. Toole, and R. Krishfield, 2018: Warming of the interior Arctic Ocean linked to sea ice losses at the basin margins. *Sci. Adv*., **4**, 1–7, https://doi.org/10.1126/sciadv.aat6773.

Toole, J. M., M. L. Timmermans, D. K. Perovich, R. A. Krishfield, A. Proshutinsky, and J. A. Richter-Menge, 2010: Influences of the ocean surface mixed layer and thermohaline stratification on Arctic sea ice in the central Canada Basin. *J. Geophys. Res.*, **115**, doi:10.1029/2009JC005660.

U.S. National Ice Center, 2018: Arctic sea ice at minimum extent. Press release. http://www.natice.noaa.gov/Main_Products.htm (accessed September 9, 2019).

INITIAL DISTRIBUTION LIST

1. Defense Technical Information Center
   Ft. Belvoir, Virginia

2. Dudley Knox Library
   Naval Postgraduate School
   Monterey, California